General Comments

This paper presents a multi-model study of changes in the Australian monsoon at the Last Glacial Maximum based on PMIP3 simulations. The topic is an important one, and the study presents interesting results showing a change in seasonality of rainfall, with increased seasonal cycle due to winter drying and early summer rainfall increases. The mechanisms producing this change are also explored, and the role of local circulation changes due to altered land configuration is identified as a major contribution to the changes.

The study fails to adequately introduce the climate models used, or to deal with the uncertainty due to model biases or model disagreement on the sign of rainfall changes. The study also employs an overly simplistic method to decompose quantitative changes in rainfall due to dynamic and thermodynamic factors, relying entirely on multi-model mean changes and using a Clausius-Clapeyron scaling that is too large for the thermodynamic component.

Despite these limitations, I believe the study could make a valuable contribution to our understanding of Australian monsoon rainfall changes under LGM conditions. Major revisions are recommended, as outlined below in my comments.

Reply to General Comments:

Thank you very much for the comments on the models' uncertainties and on the method of attribution of the changes in precipitation to dynamic and thermodynamic factors.

In the revised version, we implemented a brief discussion of the models' uncertainties along with the possible factors leading to the model biases, see Lines 380-390 in the revised text.

We have also added a short description of the decomposition method in the revised version. Please find the details in the Reply to Specific Comment 8.

We acknowledge your valuable comments and suggestions to improve our work.

Specific Comments

1. Line 69: The Australian monsoon is not defined clearly here or elsewhere, and the definition is not consistent throughout the paper or with other studies. Which domain is used? Does it include the Maritime Continent? Are land and ocean model grid points used? Is the domain the same in all models? How is the area shown in red in Figure 1a defined, and why does it include parts of the South Pacific Convergence Zone?

Note that the largest rainfall changes (Fig 1a) are over ocean to the north of Australia. If the results in this study are the area average over the grid points enclosed by the red line, then they represent mainly changes over PNG and the Maritime Continent, which makes it difficult to compare with proxy records or model studies focused on Northern Australian land areas. I suggest to re-calculate rainfall changes over Northern Australian land areas only (e.g. to 20S or 25S) and discuss and consider whether the results are consistent with those for the larger Australia-Maritime Continent domain.

Also, monsoon strength or intensity is defined in several different ways. Here (line 70) it is stated that a strong monsoon means wet conditions, whereas elsewhere a strong or intense monsoon means a large seasonal difference in rainfall between wet and dry

seasons.

Please clarify: What is the monsoon domain used? Does it include both land and ocean? How is monsoon strength and intensity defined?

Reply: The monsoon domain is defined following hydroclimate definition, i.e., a contrast between wet summer and dry winter (Wang and Ding 2008). The monsoon domain is defined by the area where the annual range (local summer minus local winter) exceeds 2.0 mm/day, and the local summer precipitation exceeds 55% of the annual total precipitation. Here in the southern hemisphere, summer means November to March and winter means May to September. Since the domains derived from different models are different, and the changes of domain are also different, we use the fixed domain derived from the merged CMAP-GPCP precipitation data. The domain includes both land and ocean areas. A brief statement has been added as the Sec. 2.3 in the revised version, Lines 173-184. Note that the monsoon domain is shown only to give a general view of precipitation change, but not the main focus of this study.

The seasonal distribution of the area averaged precipitation (Fig. 1b) is not based on the monsoon domain, but on the area where the annual range is increased, which is (20°S-EQ, 115°E-145°E) (as seen in Fig. 1a). To make it easier to compare with proxy records, the rainfall changes are re-calculated over Northern Australian land areas (20°S-5°S, 120°E-145°E) as suggested. The change in this region is different from the change in a larger region (larger Australia-Maritime Continent, i.e., 20°S-20°N, 90°E-150°E) (Fig. A). This also indicates the Australian seasonality to be a local phenomenon.

The monsoon intensity in this study is represented by the annual range or the seasonality, i.e., the local summer minus the local winter. This has been clarified throughout the revised version.

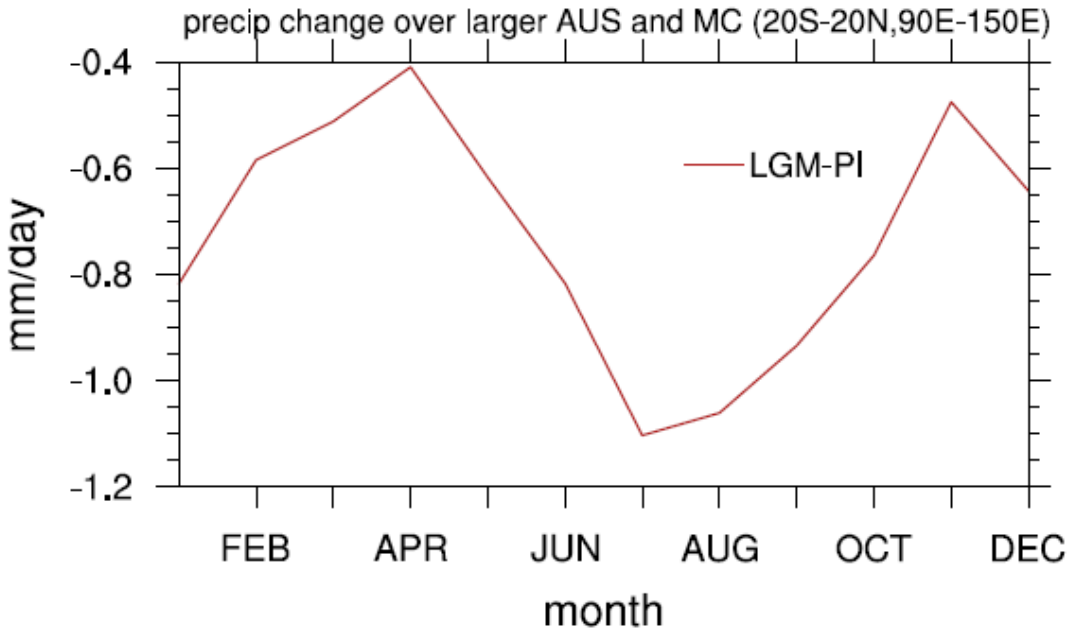

Figure A Seasonal distribution of precipitation change over the region of (20°S-20°N, 90°E-150°E). The change is calculated by P_{LGM} - P_{PI}.

2. Lines 72-75: Several of these records are not from the monsoon region, so are not relevant here.
Reply: Those unrelated papers (Treble et al. 2017; Bowler et al. 2012) are removed from the revised version, Lines 76-79.

3. Line 94: Multi-model ensembles can also provide a clearer perspective on model uncertainty (when all models agree, the result may be more robust – although not always, as models may share systematic biases).
Reply: Good point. It has been added to the revised version, Lines 94-95.

4. Lines 102-104: "This result… has not been proved yet" – it is not clear whether this discussion refers to models or proxy records. It is important to distinguish between these two sources of information, and to acknowledge that neither provides a "true" record of the LGM as proxy records require interpretation and calibration and may be spatially incomplete, while models contain biases.
Reply: Thanks for your suggestion. "This result" refers to the "simulated results", changed in the revision, Line 102. Also, "Neither model outputs nor proxy records provide a "true" record of the LGM, as proxy records require interpretation and calibration and may be spatially incomplete, while models contain biases" has been added in the revised text, Lines 104-106.

5. Line 104-107: Bayon et al. (2017) discussion of subtropics is not referring to the monsoon, which lies within the tropics. Remove or modify this sentence.
Reply: Modified, Lines 108-110.

6. Line 122: How many models were used? Comment on the model skill in simulating the Australian monsoon rainfall: the models used in PMIP3 are typically lower resolution CMIP5 models, and many do not have high skill in simulating regional rainfall. At least, cite some model evaluation studies of the Australian monsoon in CMIP5 models, e.g. Jourdain et al. (2013), Brown et al. (2016) and summarise model skill in this region.
Reply: Seven models are used in this study (Table 1), four of which have a higher resolution than 2 degrees in atmospheric component. For the oceanic component, the resolutions are even higher in six models (except IPSL). The resolutions of the oceanic components of each model have been added into Table 1 in the revised version.
The suggested references have been added to illustrate the model performance. These models' performance in the Australian monsoon region has been summarized in the revised text, see Lines 129-132.

7. Line 166: According to Held and Soden (2006), who should be cited here, global precipitation would be expected to increase (or decrease) by around 2%/K. Previous studies have found a slightly higher scaling of around 3%/K for Asian monsoon rainfall (Endo and Kitoh, 2014).
Reply: Yes, you are right. Here the 7 % change per degree of temperature change comes

from the Clausius-Clapeyron (CC) relation, which is also suggested by Held and Soden (2006). The references have been added in the revised version, Line 154 and Line 218.

8. Page 8, first paragraph: I am not comfortable with a quantitative decomposition based on the multi-model mean. The sign and magnitude of changes will be different in each model and the decomposition is only valid for individual models. Also, the scaling of precipitation with temperature is likely too strong (see point above). Further, can all these changes be considered linearly? A more robust decomposition of dynamic and thermodynamic changes in each model should be applied, e.g. Seager et al. (2010), Chadwick et al. (2013) or Endo and Kitoh (2014).

Reply: Yes, the changes are different in different models. However, we calculated the changes based on the areas where signal-to-noise ratio exceeds 1, which means this change is relatively robust among the models.

Again, the 7 % /K ratio of global precipitation over temperature comes from the Clausius-Clapeyron (CC) relation, which is also suggested by Held and Soden (2006). The actual changes are nonlinear. But we have simplified the changes as linear.

For attribution of precipitation changes, we use a simplified relation based on the linearized equation of moisture budget used in the previous works (Chou et al., 2003; Seager et al., 2010; Huang et al., 2013; Endo and Kitoh, 2014; Liu et al., 2016). Considering a quasi-equilibrium state, the vertical integrated moisture conservation can be approximately written as

$$-\int_{1000}^{0} \nabla \cdot (q\vec{v})dp = P - E \qquad (1)$$

where q is specific humidity, $\vec{v}$ is horizontal velocity, p is pressure, P is precipitation, and E the surface evaporation. Since water vapor is concentrated in the lower troposphere, the vertical integrated total column moisture divergence can be approximately replaced by the integration from the surface to 500 hPa. Define the Δ (.) as the change from PI to the LGM, i.e.,

$$\Delta(.) = (.)\mathrm{LGM} - (.)\mathrm{PI} \qquad (2)$$

Then the precipitation change $\Delta\mathrm{P}$ can be approximately calculated as follows:

$$\Delta\mathrm{P} = -\int_{p1000}^{p500} \Delta(\mathrm{q} \cdot \nabla\vec{v})dp - \int_{p1000}^{p500} \Delta(\vec{v} \cdot \nabla q)\, dp + \Delta E \qquad (3)$$

To further simplify the equation, we use $-\omega_{500}$ to represent vertical integrated $\nabla\vec{v}$, and q at the surface to represent vertical integrated specific humidity (Huang et al., 2013). Thus, the precipitation change (ΔP) can be represented as

$$\Delta\mathrm{P} \propto \bar{\omega}_{500} \cdot \Delta\mathrm{q} + \bar{\mathrm{q}} \cdot \Delta\omega_{500} + \Delta E - \Delta T_{adv} \qquad (4)$$

where $\bar{\omega}_{500}$ is 500 hPa vertical velocity in PI, $\bar{\mathrm{q}}$ is surface specific humidity in PI, ΔT_{adv} is the changes due to the moisture advection ($\int_{p0}^{p500} \Delta(\vec{v} \cdot \nabla q)\, dp$).

The first term in the right-hand side of (4) ($\bar{\omega}_{500} \cdot \Delta\mathrm{q}$) represents thermodynamic effect

(due to the change of q), and the second term ($\bar{q} \cdot \Delta\omega_{500}$) represents dynamic effect (due to the change of circulation).
The above method has been added in the revised Sec. 2.2, Lines 151-172.
The spatial distributions of each term in JJA and ND have been provided in the revised version as supplementary figures (Figure S3 and Figure S6). The descriptions are added in the revised text, Lines 227-230 and Lines 299-302.
It is clear that the dynamic effect plays more important role than the thermodynamic effect in the precipitation change over Australia and Maritime Continent. But this is not always true for other regions, such as South Africa and South America, where the thermodynamic and dynamic effects have comparable contributions.
Based on the new decomposition method, we modified the statements about the contributions of thermodynamic and dynamic effects.

9. Line 241: Where do the monsoon percentage changes come from? The rainfall changes in November-December shown in Figure 6 are in mm/day not %. The model spread (agreement) should also be discussed here and elsewhere: how many models simulate increased rainfall in the LGM and how many simulate decreased rainfall? How does this influence our confidence in the MMM changes?
Reply: The percentage of precipitation change is calculated by the difference between precipitation in LGME and in piControl divided by the climatology in piControl, i.e. $(P_{LGME} - P_{piContrl})/P_{piControl} * 100$.
Five models simulate increased local summer rainfall and the other two simulate decreased rainfall, please refer to Fig. 13 in the revised version.
We have added the area averaged results derived from each model in Table 3 in the revised version, including annual mean, local summer mean and annual range. A short summary has been added in the revised text, Lines 203-209. Since most models are in agreement, we can rely on the MME results.

10. Line 247: See point 1 above, please use a consistent definition of monsoon intensity. I suggest use "intensified seasonality" here for clarity. It is also necessary to describe in this paper how the average summer or wet season rainfall changes at the LGM, as this is the normal measure of the strength of the Australian summer monsoon. You should show (e.g. in a bar chart or table) annual mean and wet season (November to April) rainfall change for EACH model and for the MMM. This provides the context for the more detailed discussion of changes in seasonality and is more directly comparable with proxy reconstructions of annual or wet season rainfall and with studies of future monsoon (wet season) rainfall changes.
Reply: Thank you for the valuable suggestion. The seasonality is used in the revised version to represent the monsoon intensity.
As we can see from the seasonal distribution of precipitation changes derived from each model (Fig. 1c) that the largest increasing occurs in the early austral summer (ND), the simulated wet season (November to April) mean precipitation is decreased in all the models. Therefore, we take local summer (DJF) as wet season.
The annual mean, DJF mean and annual range of precipitation changes derived from

each model are listed in Table 3 in the revised version.

11. Line 258-265: The discussion of Tharammal (2017) is confusing. Do your results agree with theirs? If so, then simply state this.
Reply: Yes, our results are in agreement with theirs. The confusing part has been deleted in the revised version, Lines 316-319.

12. Line 278: Why would the precipitation change lag the insolation change by two months? Provide a reference.
Reply: In the annual variation, precipitation responds to the lower tropospheric moisture convergence. The moisture change depends on temperature change while the circulation change depends on surface temperature gradients change. The change of the surface temperature lags insolation changes because of the ocean and land surfaces have heat capacity (thermal inertial). In other words, insolation is a heating rate which equals to temperature change (tendency) but not the temperature itself.
This has been added into the revised version, see Lines 331-338.

13. Line 288: "Strong convergence rain belt": Do you mean the ITCZ?
Reply: Yes, it is related to the ITCZ. "ITCZ" is added in the revised text, Line 348.

14. Line 291: A little more northerly? It is not clear what is being compared to what here.
Reply: It is compared to the position in our study. We have clarified in the revised text, Line 350.

15. Line 309 and line 314: See discussion under point 10. State that the monsoon seasonality is amplified or intensified (rather than the monsoon itself).
Reply: Thank you again for point out the misleading statement. All have been changed into "seasonality" in the revised version. For example, Line 406 and Line 411.

16: Page 12, paragraphs 2 and 3: I repeat that I am not comfortable with a quantitative MMM decomposition. At least, you need to make it clear that your results are MMM values and state the model spread or uncertainty as well.
Reply: Changed in the revised version. The quantitative values have been removed. The model uncertainties have been concluded in Lines 437-441 in the revised text.

17. Figure 1: How is the monsoon domain defined? Why does it include the SPCZ region? Show some measure of model spread in Figure 1b, such as standard deviation of model range.
Reply: The monsoon domain is defined following Wang and Ding (2008), i.e., the areas where the annual range (local summer minus local winter) exceed 2.0 mm/day, and the ratio of local summer against annual mean precipitation exceeds 55 %. The definition has been added in the Sec. 2.3 in the revised version.
The seasonal distribution derived from each model is added as Figure 1c in the revised

version.

18. Figure 10: It may be more useful to show a smaller domain, excluding the North Pacific, with a smaller contour range. This would make the changes in Pacific and Indian Ocean tropical SSTs easier to see.
Reply: Actually, the SST change in a smaller domain was shown in Figure S4 in the original manuscript. SST change in a smaller domain has been used as Figure 10 in the revised version.

19. Figure 11: What is the "increased AR region" (11b)? What is the "central Australian monsoon region" referred to in the caption? Define the domain used.
Reply: The "increased AR region" is the "central Australian monsoon region", as shown in Fig. 1a. The region used in the revised version has been changed into North Australian land area as suggested, which is (20°S-5°S, 120°E-145°E). The figure caption has been modified in the revised version.

20: Figure 12: I am not sure if this diagram is very useful. Also, arrows (if any) and linking lines are not clear in my print version.
Reply: In the revised version, we only show the local dynamic processes in the two seasons (JJA and ND), which we think is useful for understanding the mechanisms of precipitation change. We have used thick arrows to make it clearer. The modified figure is shown in Figure 16 in the revised version.

21: Table 1: Were all model run years used from each model? This should be mentioned in Section 2. It would be more consistent to use the same number of years from each model.
Reply: Yes, we have used the same number of years for each model to get the model climatology. It has been stated in Sec. 2.1 in the revised text, Lines 133-134.

Technical Corrections
Line 85: Change wording: "The change in the Australian monsoon was inconclusive…"
Reply: Changed in the revised version, Line 84.

Line 94: Multi-model ensembles can reduce or cancel out the biases, not "delineate" (describe, define) them.
Reply: Modified in the revised version, Line 93.

Line 107: Remove "insight" before "studies".
Reply: Removed in the revised version, Line 107.

Line 110: Here and elsewhere in the paper, use "thermodynamic" not "thermal dynamic".
Reply: Yes, all have been fixed in the revised version.

Line 127: A simpler version of the PMIP3 website address is: https://pmip3.lsce.ipsl.fr/.
Reply: Yes, fixed, Line 138.

Line 151: Here and elsewhere, do not use the American term "Fall" to refer to Southern Hemisphere Autumn (use "Autumn").
Reply: All the "Fall" has been changed into "Autumn" in the revised version.

Line 159: Insert "global" before "temperature and humidity".
Reply: Yes, fixed. "global" has been added in the revised version, Line 212.

Line 205: Remove "We noticed that".
Reply: Yes, fixed, Line 231.

Line 256: It is not clear what the personal communication refers to here, I suggest remove it.
Reply: Removed in the revised version, Line 316.

Line 307: Insert "global mean" before "temperature and water vapor".
Reply: Yes, fixed. "global mean" has been added in the revision, Line 404.

Line 336: "Synthesized" does not make sense: should this be "simulated" (i.e. from models) or "multi-model mean" (i.e. averaged over many models)?
Reply: Deleted in the revised version, Line 442.

Line 469: Treble reference is incorrectly appended to Tharammal reference.
Reply: Thank you for pointing out this mistake. This redundant reference has been deleted in the revised version, Line 602.

Anonymous Referee #2

Received and published: 1 June 2018

The authors examined response of Australian monsoon to LGM forcing among CMIP5/PMIP3 multiple models. Simulated annual range of Australian monsoon rainfall during LGM is larger than present day, distinct from other regional monsoon systems. However, in a previous paper published in 2016, it has been already explored that this unique monsoon behavior was found among CMIP5/PMIP3 models and changes in land-sea contrast (due to change in land sea configuration arising from sea level drop) and east-west SST gradient are important for that. In that paper, the authors emphasized dynamic contribution to the spring-to-summer monsoon enhancement (rooted from changes in land-sea contrast and SST gradient) because thermodynamic contribution (reduced surface water vapor rooted from surface cooling) cannot explain this enhancement. Most of the contents described in the current paper are just reconfirmations of previous paper (Yan et al. 2016).

In the current paper, the authors also tried to quantify relative contributions of dynamic and thermodynamic components related to the LGM Australian monsoon response. However, their quantitative decomposition is not reasonable. They did not follow widely-accepted methodology decomposing dynamic and thermodynamic components of rainfall response under climate change based on concepts of atmospheric water vapor budget. They also simply compared model-ensemble-mean anomaly between LGM and present day and dismissed inter-model differences in regional gradients in temperature, pressure and circulation response although they are essential for their main discussion. As an overall evaluation, novelty of this study seems very limited. I would like to recommend the authors to conduct any additional tests (e.g. Chiang et al. 2003: Toracinta et al. 2004; Ueda et al. 2011) to quantify effect of the land configuration (for example) to the Australian monsoon circulation and rainfall. Such sensitivity tests in addition to the quantitative evaluation of the hydrological response in multiple models are necessary for improving quality of this study.

Reply: Thank you for your valuable and constructive comments for improving our study.

In the revised version, we have added the decomposing method to assess the hydrological response and have added two additional simulations to test the effect of land-sea configuration on Australian monsoon.

Please find the detailed method of quantitative assessment of the hydrological response in the Reply to Comment 1.

The additional simulations have been added in the Discussion Section in the revised text. To isolate the impacts of land-sea configuration change, two experiments are conducted using a fully coupled earth system model (NESM v1, Cao et al., 2015). One is the PI control run designed the same as PMIP3 protocol, the other is the same

as PI control run but with LGM land-sea configuration. The sensitive simulation illustrates that the local dynamical process induced by the land-sea configuration change is essential to the Australian monsoon precipitation change. The additional simulated results are shown in Figure 12 in the revised version. The additional simulations and results are included in the Discussion Section, Lines 365-379.

Other comments

1. *Please follow commonly-used dynamic-thermodynamic decomposition method. In line 165-173, 183-191 and other parts, ratio of specific humidity change should not be simply converted to that of precipitation change. Please read carefully Held and Soden 2006, O'Gorman et al. 2012 to catch current understanding of response of hydrological cycle under climate change, and Chou et al. 2009, Seager et al. 2010, and Chadwick et al. 2013 to understand widely-accepted methods for decomposition of dynamic and thermodynamic contributions to rainfall response under different climate states.*

Reply: Thank you for your suggestion. In the revised work, we have made a rigorous quantitative analysis of the precipitation response to dynamic and thermodynamic factors.

For attribution of precipitation changes, we use a simplified relation based on the linearized equation of moisture budget used in the previous works (Chou et al., 2003; Seager et al., 2010; Huang et al., 2013; Endo and Kitoh, 2014; Liu et al., 2016). Considering a quasi-equilibrium state, the vertical integrated moisture conservation can be approximately written as:

$$-\int_{1000}^{0} \nabla \cdot (q\vec{v})dp = P - E \qquad (1)$$

where q is specific humidity, $\vec{v}$ is horizontal velocity, p is pressure, P is precipitation, and E the surface evaporation. Since water vapor is concentrated in the lower troposphere, the vertical integrated total column moisture divergence can be approximately replaced by the integration from the surface to 500 hPa. Define the Δ (.) as the change from PI to the LGM, i.e.,

$$\Delta(.) = (.)\mathrm{LGM} - (.)\mathrm{PI} \qquad (2)$$

Then the precipitation change $\Delta\mathrm{P}$ can be approximately calculated as follows:

$$\Delta\mathrm{P} = -\int_{p1000}^{p500} \Delta(\mathrm{q} \cdot \nabla\vec{v})dp - \int_{p1000}^{p500} \Delta(\vec{v} \cdot \nabla q)\, dp + \Delta E \qquad (3)$$

To further simplify the equation, we use $-\omega_{500}$ to represent vertical integrated $\nabla\vec{v}$, and q at the surface to represent vertical integrated specific humidity (Huang et al., 2013). Thus, the precipitation change (ΔP) can be represented as

$$\Delta\mathrm{P} \propto \bar{\omega}_{500} \cdot \Delta\mathrm{q} + \bar{\mathrm{q}} \cdot \Delta\omega_{500} + \Delta E - \Delta T_{adv} \qquad (4)$$

where $\bar{\omega}_{500}$ is 500 hPa vertical velocity in PI, $\bar{\mathrm{q}}$ is surface specific humidity in PI, ΔT_{adv} is the changes due to the moisture advection ($\int_{p0}^{p500} \Delta(\vec{v} \cdot \nabla q)\, dp$).

The first term in the right-hand side of (4) ($\bar{\omega}_{500} \cdot \Delta\mathrm{q}$) represents thermodynamic effect

(due to the change of q), and the second term ($\bar{q} \cdot \Delta\omega_{500}$) represents dynamic effect (due to the change of circulation).

The above method has been added in the revised Sec. 2.2, Lines 151-172.

The spatial distributions of each term in JJA and ND have been provided in the revised version as supplementary figures (Figure S3 and Figure S6). The descriptions are added in the revised text, Lines 227-230 and Lines 299-302.

It is clear that the dynamic effect plays more important role than the thermodynamic effect in the precipitation change over Australia and Maritime Continent. But this is not always true for other regions, such as South Africa and South America, where the thermodynamic and dynamic effects have comparable contributions.

Based on the new decomposition method, we modified the statements about the contributions of thermodynamic and dynamic effects.

2. *Please show inter-model consistency in (1) regional gradient in surface temperature, sea level pressure and rainfall, and (2) east-west SST gradient. In this paper, the authors checked inter-model consistency in LGM anomaly compared to PI. However, inter-model consistencies in the regional gradients in LGM anomaly (for example, are east-west dSST gradients really consistent among 7 models?) are not accessed although they are essential for the conclusion.*

Reply: The inter-model consistencies of regional gradient in temperature, SLP and SST have been provided in the revised version as supplementary (Figure S5).

The east-west SST gradient (warm western tropic Pacific Ocean and cold eastern tropic Indian Ocean) is consistent among the models, please refer to the Figure S5e.

3. *Please check inter-model consistency in LGM land configuration. Although the LGM land configuration was specified in PMIP3 protocol, land configuration implemented in each model could be different because model resolutions are much different between different model. Land-sea mask data in native grid of each model should be checked because any inter-model difference possibly affect inter-model difference in results.*

Reply: Although the resolutions of atmospheric component in each model are much different, four of the seven models have higher resolutions than 2-degree. For the oceanic component, most models (except IPSL-CM5A-LR) have higher resolutions than 1-degree. We have added the resolutions used in the oceanic component of the models in Table 1.

It's hard to obtain the land-sea mask data from each model, here we use the climatology of SST in the LGM to illustrate the land-sea configuration in each model (Figure A). We are focusing on the tropical Indian Ocean and tropical west Pacific Ocean. Note that the resolution of 7MME is 2.5°*2.5°, lower than the individual models.

The resolution of land configuration might not be the key question that will affect the results.

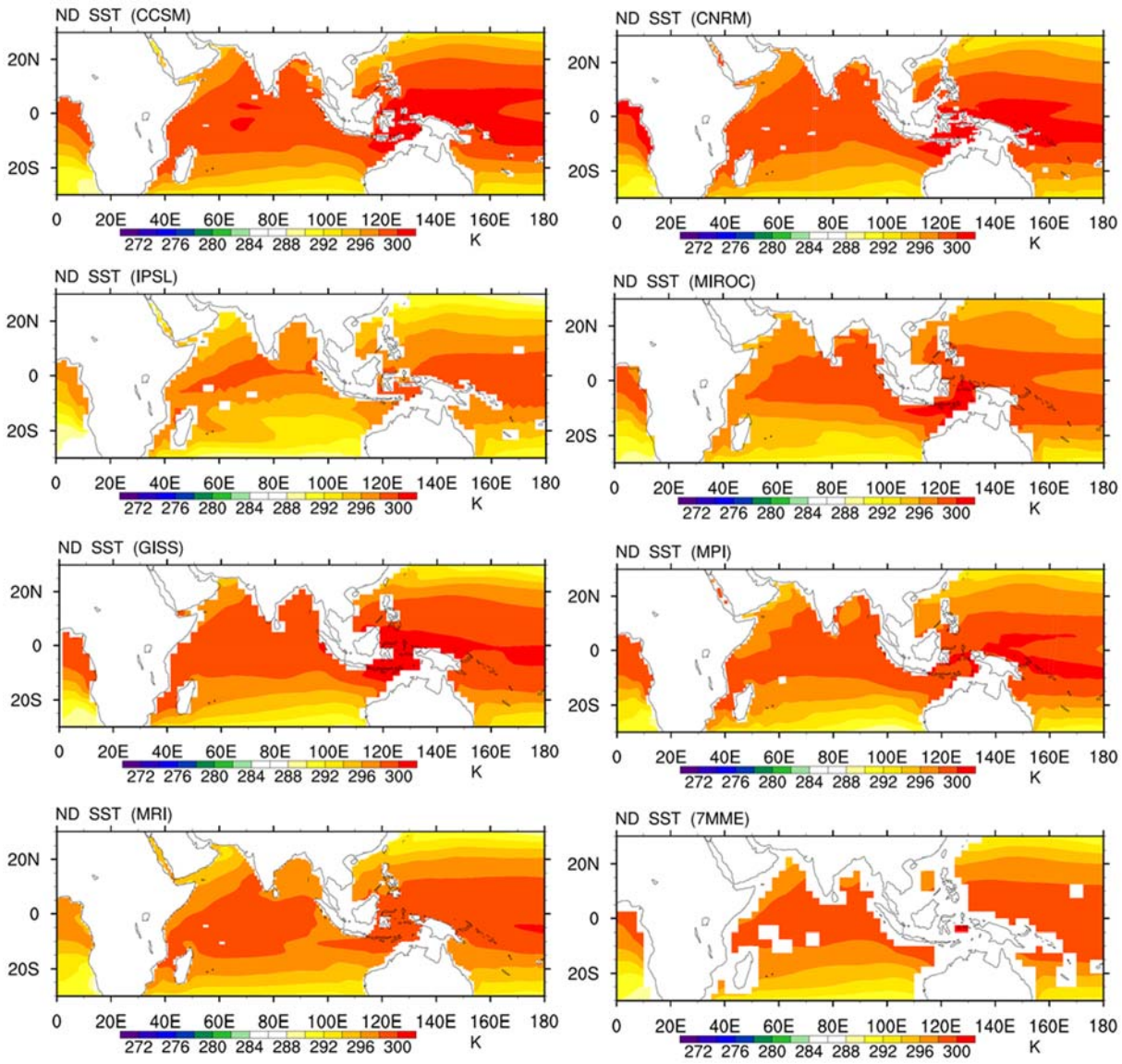

Figure A ND mean SST in LGME derived from each model and 7MME.

4. *Figures S1 and S2 seem identical to Figures 2 and 1 of Yan et al. (2016). You may need any copyright permission from Springer-Nature.*

Reply: The paper of Yan et al. (2016) has been purchased "Open Access" in Climate Dynamics. So, we don't need to obtain the copyright.

5. *Line 26: relative -> related?*

Reply: Yes, it should "be related", changed in the revised version. Please refer to Line 26 in the revised text.

6. *Line 41-44: I couldn't catch what do you mean here. Are "the local processes" you mention here land-sea configurations?*

Reply: Some synthesis suggests that the change of Australian monsoon during the

LGM might be related to the large-scale circulation change such as the shifted position of ITCZ. However, in this work we find that it is not closely related to this large-scale circulation change, but to the local dynamics.
In this study, "the local dynamics" not only represents the dynamics due to the "land-sea contrast", but also due to the "asymmetric SST changes between the east tropical Indian Ocean and tropical western Pacific Ocean".
The statement has been modified in the revised version as follows:
“The enhanced Australian monsoonality in the LGM is not associated with global scale circulation change such as the shift of the ITCZ, rather, it is mainly due to the change of regional circulations around Australia arising from the changes in land-sea contrast and the east-west SST gradients over the Indo-western Pacific oceans. This finding should be taken into account …” Please refer to Lines 42-45.

7. *Line 110: thermal dynamics -> thermodynamic*

Reply: Thank you for pointing out this. All the terms of "thermal dynamics" have been changed into "thermodynamics" in the revised version.

Understanding the Australian Monsoon change during the Last Glacial Maximum with multi-model ensemble

Mi Yan[1,2], Bin Wang[3,4], Jian Liu[1,2*], Axing Zhu[1,2,5,6], Liang Ning[1,2,7] and Jian Cao[4] ~~and Liang Ning[1,2,7]~~

1 Key Laboratory of Virtual Geographic Environment, Ministry of Education; State key Laboratory of Geographical Environment Evolution, Jiangsu Provincial Cultivation Base; School of Geography Science, Nanjing Normal University, Nanjing, 210023, China.

2 Jiangsu Center for Collaborative Innovation in Geographical Information Resource Development and Application, Nanjing, 210023, China.

3 Department of Atmospheric Sciences, University of Hawaii at Manoa, Honolulu, HI 96825, USA.

4 Earth System Modeling Center, Nanjing University of Information Science and Technology, Nanjing, 210044, China.

5 State Key Lab of Resources and Environmental Information System, Institute of Geographic Sciences and Natural Resources Research, Chinese Academy of Sciences, Beijing, 100101, China

6 Department of Geography, University of Wisconsin-Madison, Madison, WI 53706, USA

7 Climate System Research Center, Department of Geosciences, University of Massachusetts, Amherst, 01003, USA.

* Corresponding author address: Dr. Jian Liu, School of Geography Science, Nanjing Normal University, 1 Wenyuan Road, Nanjing 210023, China

E-mail: jliu@njnu.edu.cn

Abstract

The response of Australian monsoon to the external forcings and the ~~relative~~ related mechanisms during the Last Glacial Maximum (LGM) is investigated by multi-models' experiments in CMIP5/PMIP3. Although the annual mean precipitation over the Australian monsoon region decreases, the annual range, or the monsoonality, is enhanced. The precipitation increases in early austral summer and decreases in austral winter, ~~causing~~ resulting in the amplified annual range, but ~~or monsoonality to amplify.~~the main contribution comes from the ~~The~~ decreased precipitation in austral winter ~~has a large contribution to the strengthened monsoonality~~. ~~It~~The decreased winter precipitation is primarily caused by ~~the~~ weakened upward motion, although ~~the~~ reduced water vapor has also a moderate contribution. The weakened upward motion ~~in austral winter~~ is induced by the enhanced land–sea thermal contrast, which intensifies the divergence over the northern Australia. The increased Australian monsoon rainfall in early summer, on the other hand, is an integrated result of the positive effect of local dynamic processes (enhanced moisture convergence) and the negative effect of thermodynamics (reduced moisture content). The enhanced moisture convergence is caused by two factors: the strengthened northwest–southeast thermal contrast between the cooler Indochina–western Indonesia and the warmer northeastern Australia, and the east–west sea surface temperature gradients between the warmer western Pacific and cooler eastern Indian Ocean, both due to the alteration of land–sea configuration arising from the sea level drop. The enhanced Australian monsoonality in the LGM is not associated with global scale circulation change such as the shift of the ITCZ, rather, it is mainly due to the change of regional circulations around Australia arising from the changes in land-sea contrast and the east-west SST gradients over the Indo-western Pacific oceans. ~~caused by the local processes rather than the large scale dynamics, which~~ This finding should be taken into account when investigating its future change under global warming. Our findings may also explain why proxy records indicate different changes in Australian monsoon precipitation during the LGM.

1 Introduction

The changes of the Australian monsoon are crucial for human society and ecology in Australia (Reeves et al., 2013a), considering the socio-economic importance of monsoon rainfall (Wang et al., 2017). As the monsoons of the summer hemisphere are linked via outflows from the opposing winter hemisphere, the Australian monsoon can also influence the Asian–Indonesian–Australian monsoon system (Eroglu et al., 2016). It is important to understand how and why the Australian monsoon would change in response to global climate change.

With strong climatic forcings (including low greenhouse gas (GHG) concentrations, large ice-sheets, and low sea level, etc.), the Last Glacial Maximum (LGM) is one of the key periods that provides an opportunity to better understand the mechanisms of how global and regional climate ~~response~~ respond to external forcings (Hewitt et al., 2001; Braconnot et al., 2007; Braconnot et al., 2011; Harrison et al., 2014). Previous studies have investigated how the external forcing and boundary conditions during the LGM affected the Intertropical Convergence Zone (ITCZ) ~~location~~ (Broccoli et al., 2006; Donohoe et al., 2013; McGee et al., 2014), the Walker circulation (DiNezio et al., 2011), the Indo-Pacific climate (Xu et al., 2010; DiNezio and Tierney, 2013; DiNezio et al., 2016), the SH circulation (Rojas, 2013), and the global monsoon (Jiang et al., 2015; Yan et al., 2016). The Australian monsoon onset and variability during the post-glacial, the late deglaciation, and the Holocene have also been studied using proxy datasets (Ayliffe et al., 2013; De Deckker et al., 2014; Kuhnt et al., 2015; Bayon et al., 2017). However, due to the limitation of the scarce proxy datasets, the Australian monsoon change during the LGM is far from clearly understood.

There are different proxy evidences indicating different Australian monsoon change during the LGM. Here, the Australian monsoon intensity is ~~defined based on~~represented by the seasonality of precipitation, i.e., a stronger ~~(weak)~~ monsoon means a wetter ~~(dry) condition~~summer and/or drier winter. Some records show wet conditions over Australia during the LGM (Ayliffe et al., 2013), while other proxies indicate drier conditions (Denniston et al., 2013; Denniston et al., 2017; DiNezio and Tierney, 2013). The isotopes from eggshell of five regions across Australia affirms that Australia becomes drier in the LGM (Miller et al., 2016), while the ~~speleothem records of southern Australia indicate that it is relatively wet during the LGM (Treble et al., 2017). The~~ archaeological record showed a refugia-type hunter-gatherer

response over northwest and northeast Australia during the LGM (Williams et al., 2013), indicating that these areas may have had a wetter summer and were therefore preferred by people as refugia. ~~Bowler et al. (2012) found that the desert dunes advanced while people upstream feasted on fish and shellfish during the LGM when investigating the lake records over the southern Australia.~~ The synthesis by the OZ-INTIMATE (Australian INTIMATE, INTegration of Ice core, MArine and TErrestrial records) project (Turney et al., 2006; Petherick et al., 2013) showed that the palaeoenvironment over Northern Australia during the LGM was characterized by drier conditions although wet periods were also noted in the fluvial records (Reeves et al., 2013a; Reeves et al., 2013b).

The change in the Australian monsoon was ~~As one can see from the above description, it is~~ inconclusive ~~on the Australian monsoon change~~ during the LGM based on proxy data. Therefore, scholars started investigating the Australian monsoon change from numerical simulation perspectives. The sensitivity of Australian monsoon to forcings during the late Quaternary has been analyzed using simulations by Fast Ocean Atmosphere Model (Marshall and Lynch, 2006, 2008). Numerical experiments have been conducted to analyze the impacts of obliquity and precession with a coupled General Circulation Model (Wyrwoll et al., 2007) and orbital time-scale circulation with Community Climate Model (Wyrwoll et al., 2012) on the Australian monsoon. However, different models may have different responses to the same external forcings, such that the simulated results may have model dependence. Multi-model ensemble (MME) can ~~delineate~~ reduce the model biases and therefore provide more reasonable results of how and why climate system responds to the external forcing changes. The MME can also provide a clearer perspective on model uncertainties.

Yan et al (2016) thus used the multi-model ensemble approach to examine the response of global monsoon to the LGM conditions. It was found that the global monsoon and most sub-monsoons weakened under the LGM conditions. Some brief hypothesis was made to explain the changes from global and hemispheric perspectives. The Australian monsoon was thought to be strengthened due to the southward shift of the ITCZ resulted from the hemispheric thermal contrast and due to the land-sea thermal contrast resulted from the land-configuration. However, this ~~qualified~~ simulated result of strengthened monsoon or wet condition has not been proved yet. As mentioned above, it is inconclusive whether the Australian monsoon is strengthened or not during the LGM, due to the limitations of proxies' and models' uncertainties. Neither model

outputs nor proxy records provide a “true” record of the LGM, as proxy records require interpretation and calibration and may be spatially incomplete, while models contain biases. ~~Moreover, Bayon et al. (2017) suggested that the rainfall pattern in subtropical Australia during the last glacial period was modulated by additional mechanisms rather than simply the ITCZ.~~ Therefore, model-data and inter-model comparison are needed and ~~insight~~ studies on the mechanisms are required to better understand the Australian monsoon change during the LGM. Moreover, some studies show that the Australian climate during the last glacial period was modulated by additional mechanisms rather than simply the ITCZ（Bayon et al., 2017). Thus, single forcing runs are also required to figure out the contributions of different forcings.

This paper ~~will~~ investigates the Australian monsoon change during the LGM and its mechanisms from both ~~thermal dynamics~~thermodynamics and dynamics perspectives, using the multi-model ensemble mean derived from models in the fifth phase of the Coupled Model Intercomparison Project (CMIP5) (Taylor et al., 2012) and the third phase of the Paleoclimate Modeling Intercomparison Project (PMIP3) (Braconnot et al., 2012). We are also trying to quantify the contributions of the ~~thermal~~ thermodynamic~~al~~ and the dynamic~~al~~ processes to the Australian monsoon change during the LGM. Additionally, we are applying single forcing run to test the effect of land-configuration as mentioned in Yan et al. (2016). The models and experiments used in this paper are introduced in Sect. 2. Section 3 describes simulated results and the physical mechanisms. The comparison with proxies and other simulations is discussed in Sect. 4 and the conclusions are made in Sect. 5.

2 ~~Model and Experiments~~Methods

2.1 Model and experiments

带格式的: 字体: 非加粗

Two experiments performed by models participating in CMIP5/PMIP3 are compared in this paper: the Last Glacial Maximum Experiment (LGME) and the pre-industrial (PI) control run (piControl). The models and experiments are listed in Table 1, including 7 models and 2 experiments. The models contributed to CMIP5 have been evaluated in the previous studies to have good performance in simulating the Australian monsoon precipitation seasonality or

seasonal cycle (Jourdain et al., 2013; Brown et al., 2016), which is used to represent the Australian monsoon intensity in this study.

The last 100 years of the LGME and the last 500 years of the piControl from each model are used to illustrate the model climatology. To obtain the multi-model ensemble (MME), the model outputs were interpolated into a fixed 2.5° (latitude) × 2.5° (longitude) grid using the bilinear interpolation method.

The LGM external forcing and boundary conditions are listed in Table 2. More specific documentation can be found on the PMIP3 website (https://~~wiki~~pmip3.lsce.ipsl.fr~~/pmip3/doku.php/pmip3:design:21k:final~~).

Compared with the PI, during the LGM the Southern Hemisphere (SH) low latitudes (30°S-EQ) receive more insolation from January to August and less from August to December. The NH low latitudes (EQ-30°N) receive less insolation from June to October and more from November to May (Fig. S1). Due to the decreased sea level, the landmasses expanded during the LGM. A land bridge formed between Indochina and western Indonesia, and the Arafura Sea between New Guinea and Australia closed and became landmass (Fig. S2).

To illustrate the robust changes simulated by the different models, ~~T~~the signal-to-noise ratio (S2N) test is used ~~to illustrate the robust changes simulated by the different models~~. The S2N is defined by the ratio of the absolute mean of the MME (as the signal) to the averaged absolute deviation of the individual model against the MME (as the noise) (Yan et al., 2016). In the following sections, we only consider the areas in which the S2N ratio exceeds one when we examine the differences between ~~the results derived from~~ the LGME and piControl derived from the MME.

2.2 Decomposition method

For attribution of precipitation changes, we use a simplified relation based on the linearized equation of moisture budget used in the previous works (Chou et al., 2009; Seager et al., 2010; Huang et al., 2013; Endo and Kitoh, 2014; Liu et al., 2016). Considering a quasi-equilibrium state, the vertical integrated moisture conservation can be written as:

$$-\int_{1000}^{0}\nabla\cdot(q\vec{v})dp = P - E \quad (1)$$

域代码已更改

带格式的: 首行缩进: 3 字符

带格式的: 缩进: 首行缩进: 0 厘米

带格式的: Text, 行距: 1.5 倍行距

带格式的: 字体: (中文) 宋体, (中文) 中文(中国), 检查拼写和语法

带格式的: 字体: (中文) 宋体, 字体颜色: 自动设置, (中文) 中文(中国)

带格式的: 字体颜色: 自动设置

带格式的: 字体颜色: 自动设置

带格式的: 字体颜色: 自动设置

带格式的: 字体颜色: 自动设置

带格式的: 字体颜色: 自动设置

带格式的: 字体颜色: 自动设置

带格式的: 字体颜色: 自动设置

where q is specific humidity, $\vec{v}$ is horizontal velocity, p is pressure, P is precipitation, and E the surface evaporation. Since water vapor is concentrated in the lower troposphere, the vertical integrated total column moisture divergence can be approximately replaced by the integration from the surface to 500 hPa. Define the Δ (.) as the change from PI to the LGM, i.e.,

$$\Delta(\ ) = (\ )_{\mathrm{LGM}} - (\ )_{\mathrm{PI}} \quad (2)$$

Then the precipitation change ΔP can be calculated as follows:

$$\Delta P = -\int_{p1000}^{p500} \Delta(q \cdot \nabla\vec{v})dp - \int_{p1000}^{p500} \Delta(\vec{v} \cdot \nabla q)\, dp + \Delta E \quad (3)$$

To further simplify the equation, we use $-\omega_{500}$ to represent vertical integrated $\nabla\vec{v}$, and q at the surface to represent vertical integrated specific humidity (Huang et al., 2013). Thus, the precipitation change (ΔP) can be represented as

$$\Delta P \propto \bar{\omega}_{500} \cdot \Delta q + \bar{q} \cdot \Delta\omega_{500} + \Delta E - \Delta T_{adv} \quad (4)$$

where $\bar{\omega}_{500}$ is 500 hPa vertical velocity in PI, $\bar{q}$ is surface specific humidity in PI, ΔT_{adv} is the changes due to the moisture advection ($\int_{p0}^{p500} \Delta(\vec{v} \cdot \nabla q)\, dp$).

The first term in the right-hand side of (4) ($\bar{\omega}_{500} \cdot \Delta q$) represents thermodynamic effect (due to the change of q), and the second term ($\bar{q} \cdot \Delta\omega_{500}$) represents dynamic effect (due to the change of circulation).

2.3 Monsoon domain

The monsoon domain is defined following hydroclimate definition, i.e., a contrast between wet summer and dry winter (Wang and Ding 2008). The monsoon domain is defined by the area where the annual range (local summer minus local winter) exceeds 2.0 mm/day, and the local summer precipitation exceeds 55% of the annual total precipitation. Here in the southern hemisphere, summer means November to March and winter means May to September. Since the domains derived from different models are different, and the changes of domain are also different, we use the fixed domain derived from the merged Climate Prediction Center Analysis of Precipitation (CMAP, Xie and Arkin, 1997) and Global Precipitation Climatology Project (GPCP, Huffman et al., 2009) data.

Note that the monsoon domain is shown to give a general view of precipitation change, but not the purpose of this study.

带格式的: Text, 行距: 1.5 倍行距
带格式的 ... [1]
带格式的 ... [2]
带格式的: 居中
带格式的: Text, 行距: 1.5 倍行距
带格式的 ... [3]
带格式的 ... [4]
带格式的 ... [5]
带格式的: Text, 行距: 1.5 倍行距
带格式的 ... [6]
带格式的: Text, 行距: 1.5 倍行距
带格式的 ... [7]
带格式的 ... [8]
带格式的 ... [9]
带格式的 ... [10]
带格式的: 缩进: 首行缩进: 0 厘米
带格式的 ... [11]
带格式的 ... [12]
带格式的 ... [13]

3 Results

We defined the difference of precipitation rate between austral summer (DJF) and austral winter (JJA) as the annual range ~~(AR)~~, i.e. the seasonality, to measure the monsoonality of the Australian monsoon. An increased annual range (or seasonality) means a strengthened monsoonality. Unlike the South African and South American monsoon regions (not shown), the monsoonality of the Australian monsoon derived from the seven models' multi-model ensemble (7MME) is strengthened during the LGM (Fig. 1a). This amplified annual range is the result of increased precipitation in austral summer and decreased precipitation in austral winter (Fig. 1b). Note that the largest decrease in precipitation occurred from April to July (late autumn to early winter), not exactly in austral winter; and the largest increase of precipitation occurred in November and December (ND), i.e., austral early summer. Since the amount of ~~fall~~autumn–winter reduction of precipitation exceeds the increased precipitation in early summer, the annual mean precipitation over the strengthened ~~AR~~ annual range region decreases (by 0.36 mm/day). In summary, while the total annual precipitation decreases in the LGM, the ~~AR~~ annual range (or the ~~intensity~~seasonality) of the Australian monsoon rainfall is amplified due to seasonal redistribution of the precipitation, especially the drying in austral ~~fall~~ autumn (April–May) and winter (JJA) over Australia.

Although there are model biases, most of the models (except MPI-ESM-P) simulate an enhanced annual range (or seasonality/monsoonality) in the central Australian monsoon region (20°S-5°S, 120°E-145°E) (Table 3 and Fig. 1c). Most of the models (except CNRM-CM5 and MPI-ESM-P) also simulate an increased summer precipitation over that region. All the models simulate decreased precipitation from April to September (Fig. 1c). On the other hand, the simulated annual mean precipitation is decreased in most models, except GISS-E2-R. The model uncertainties will be discussed later in Sec. 4.

3.1 Reasons for the decreased precipitation during the LGM in austral winter (JJA)

During the LGM, the lower GHG concentration and the large ice-sheets are the primary causes for the decreased global temperature and the humidity. The global surface specific humidity is reduced by 2 g/kg (or 20 %) in JJA during the LGM, compared with the PI. For the SH monsoon regions, the surface specific humidity is ~~more~~ reduced more over the Australian

monsoon region ~~(by 3.4 g/kg, or 25 %)~~ than over the other two monsoon regions of South Africa and South America (Fig. 2).

As suggested by the Clausius–Clapeyron ~~equation~~relation (C-C relation), one degree of temperature decrease would lead to about a 7 % decrease in the saturation water vapor (Held and Soden, 2006), or roughly the same scale of decrease in the ~~column integrated water vapor~~low tropospheric specific humidity. If the circulation, evaporation and advection remains unchanged, the precipitation should also be reduced by 7 % with regard to the equation (4). During the LGM, the simulated near surface air temperature over the central Australian monsoon region (20°S-5°S, 120°E-145°E) decreases significantly by 2.5 K in JJA, which implies a decrease of about 17 % resulted from the C-C relation. However, the simulated precipitation in the LGM is reduced by 1.~~16~~45 mm/day or ~~58~~44 % comparing to the PI, which is far beyond the value suggested by the thermodynamic effect (approximately 17 %). This suggests that the majority of the reduction in winter precipitation is due to the changes of ~~circulation~~ rest terms in equation (4), including the circulation change (dynamics), the evaporation change and the change due to the advection term~~changes~~. The changes of each terms show that the circulation change plays a dominant role in the precipitation change over Australia (Fig. S3). The change due to the evaporation is also important. The change due to the advection term is negligible.

The change of the surface wind field shows a strengthened divergence pattern over the Australian monsoon region (Fig. 3a, vector), which is consistent with the strengthened descending flow over the Australian monsoon region (Fig. 4) and thus reduced precipitation (Fig. 3a, shading).

The JJA mean near surface air temperature shows that the land is cooler than the adjacent ocean around northern Australia (Fig. 5a), which illustrates a strengthened land–sea thermal contrast because the land cools more than the ocean surface during the LGM. This strengthened land–sea contrast leads to a higher sea-level pressure (SLP) over land and lower SLP over ocean in general (Fig. 5b, shading), and thus the outflows from land (Fig. 5b, vector). The geopotential height at 850 hPa also shows the relative pattern that matches the wind change (Fig. ~~S3a~~S4a). The difference of divergence/convergence field (Fig. 5c) also indicates that the divergence at 850 hPa over the northern Australia is strengthened during the LGM. The ~~divergence~~ vertical

velocity at 500 hPa over the central Australian monsoon region (20°S-5°S, 120°E-145°E) illustrates that the descending flow strengthened ~~northern Australia increased~~ by about 48 %.

~~According to the surface rainfall equation, the precipitation is proportional to the water vapor content and the low-level convergence (Cui, 2009). Roughly speaking, during the LGM, the water vapor content is only 80 % of the PI, while the low-level convergence is only 52 % of the PI, thus the anticipated precipitation should be 80 % × 52 % = 41.6 %. This means the anticipated precipitation will decrease by 58.4 %, which is close to the 58 % of the decrease in the simulated precipitation.~~ In conclusion, both the dynamic process (increased subsidence) and the thermodynamic process (reduced water vapor content) contribute to the drier winter in the Australian monsoon region, but the local dynamic processes play a dominant role in the reduction of Australian winter precipitation.

3.2 Why the precipitation increased in austral early summer (ND)

During ND, the LGM minus PI surface wind difference field shows a strengthened convergence pattern over the central northern Australian monsoon region (Fig. 6a, vector), which is consistent with the increased precipitation (Fig. 6a, shading). The vertical velocity at 500 hPa also shows a strengthened ascending flow over this area (Fig. 7). The increased precipitation over the central Australian monsoon region is clearly against the thermodynamic effects of the low GHG concentration and the presence of the ice-sheets, which tends to reduce the precipitation. The 2-m air temperature was decreased by 2.2 K and the surface specific humidity reduced by 2.6 g/kg (or 16.0 %) over the Australian monsoon region (Fig. 8). The precipitation would decrease by 15.4 % according to the thermal effect without the circulation change. However, the precipitation over the Australian monsoon region increased by about 13.0 %. Therefore, the changes in dynamic processes must induce a 29 % increase of precipitation, so that the net increase in precipitation reaches 13 %.

~~We noticed that t~~There is a cyclonic wind anomaly associated with an anomalous low pressure over the northwest Australia (Fig. 6a and Fig. 9b, vector), accompanied by a strengthened low-level convergence (Fig. 9c), which favors increased precipitation in the Australian monsoon region. The change of the moisture transport (moisture flux) also indicated increased moisture transport into northern Australia (not shown). The cyclonic vorticity in

northwest Australia is partially caused by the enhanced strong low-level westerlies that prevail north of Australia.

We now seek to determine why there was a strengthened low-level westerly with maximum over north of Australia. We first consider the temperature change. The ND mean 2-m air temperature during the LGM shows that the two enlarged landmasses over the Indo-Pacific warm pool region (resulting from the lower sea level) change differently (Fig. 9a). It is cooler over the northwest landmass (western Indonesia–Indochina) and relatively warmer over the southeast landmass (eastern Indonesia–northern Australia). This temperature variation forms a southeast–northwest temperature gradient (Fig. 9a, Fig. S5a, S5b), accompanied by a northwest–southeast SLP gradient (Fig. 9b, Fig. S5c, S5d). The northwest–southeast pressure gradient is stronger in the geopotential height change at 850 hPa (Fig. ~~S3b~~S4b). The high pressure in the western Indonesia–Indochina is a part of the larger scale enhanced winter monsoon over the South China Sea. This enhanced winter monsoon flows cross the equator from the NH to the SH and turn into strong westerlies due to deflection induced by the Coriolis force. The 850 hPa convergence strengthens over the Australian monsoon region (Fig. 9c), and the corresponding ascending motion at 500 hPa also increases over the Australian monsoon region.

Another reason for circulation change is the sea surface temperature (SST) gradient change. The SST anomaly in ND shows a warmer Western Pacific and cooler Eastern Indian Ocean pattern (Fig. 10), indicating a westward temperature gradient (Fig. S5e), and thus an eastward pressure gradient which, in the equatorial region, can directly enhance westerly winds near the northern Australian monsoon region (Fig. 9b). Li et al. (2012) also found that a cold state of the Wharton Basin (100°E–130°E, 20°S–5°S) was accompanied by anomalous westerlies and cyclonic circulation anomalies in the Australian monsoon region, which were associated with a strong tropical Australian summer monsoon and enhanced rainfall over northeast Australia.

In summary, during ND, the enlarged land area due to sea-level drop enhances the land–sea thermal contrast, and forms a northwest–southeast thermal contrast which induces low pressure over northern Australia but high pressure over the adjacent ocean and the Indochina–western Indonesia, leading to enhanced convergence over northern Australia and thus increasing the early summer monsoon rainfall. The SST gradients between the warm equatorial western

Pacific and relatively cool eastern Indian Ocean during the pre-summer monsoon season also contribute to the strengthened equatorial westerlies and the cyclonic wind anomaly over northern Australia. These dynamic mechanisms have a positive contribution to the early summer precipitation ~~(nearly 29 %)~~. The thermal effects have negative contribution to the precipitation change, but with smaller impact ~~by about 16 %~~. Therefore, the early summer precipitation over northern Australia increases ~~by about 13 %~~. We can also tell from the changes of the decomposed terms that the dynamics plays much more important role in the precipitation change over Australia, especially the distribution pattern (Fig. S6). Again, the impacts of evaporation and advection terms are small.

4 Discussion

The intensification of the Australian monsoon in this study is measured by the enhanced seasonal difference (or the seasonality) of precipitation, and is particularly attributed to the decreased austral winter precipitation. This is consistent with the reconstructed results by Mohtadi et al. (2011), which indicated that it was not significantly drier in austral summer during the LGM, while (the winter monsoon is weakened). Whereas the annual mean precipitation is decreased, which means the Australian monsoon would be weakened during the LGM when it is measured by the annual mean precipitation. The modeling study by DiNezio et al. (2013) suggests a decreasing rainfall across northern Australia during the LGM, consistent with the proxy synthesis by stalagmite (Denniston et al., 2017). The decreased rainfall in their work represents the annual mean precipitation, which also consists with our work in this point of view. On the other hand, the increased rainfall in austral summer in this study is consistent with what has been revealed in the reconstructed work by Liu et al. (2015) ~~(Shen CC, personal communication, 2017)~~.

带格式的: 突出显示

The decreased annual mean precipitation and the intensified seasonality of precipitation over the Australian monsoon region ~~is~~ are in agreement with the synthesis from the simulated result by Tharammal et al. (2013) using a set of experiments. ~~In their work, the seasonality is calculated by the difference between boreal summer (JJA) and boreal winter (DJF), and the difference of the seasonality over the Australian monsoon region between the LGM and the PI is negative. Regarding to their negative value during the PI, the seasonality of precipitation over the~~

~~Australian monsoon region is actually enhanced during the LGM, which also indicates an intensified Australian monsoon.~~

For the forcings and mechanisms of the Australian monsoon change during the LGM, there are large changes in four external forcings during the LGM, including the insolation change resulting from the orbital change, the land–sea configuration change, the GHG change and the presence of ice-sheets. The lower GHG concentrations and the presence of ice-sheets are likely to be contributors to the thermal effect leading to the reduced water vapor and thus the decreased rainfall both in austral winter and early summer. The enlarged the landmasses over western Indonesia and northeastern Australia are essential to the local dynamic processes that influence the rainfall. The low obliquity and high precession during the LGM may be another factor that can affect the rainfall (Liu et al., 2015). However, the impact of the insolation change caused by the orbital change remains unknown.

During the LGM, the insolation over tropical region increased from December to June and decreased from July to November (Fig. 11a). In the annual variation, precipitation responds to the lower tropospheric moisture convergence. The moisture change depends on temperature change while the circulation change depends on surface temperature gradients change. The change of the surface temperature lags insolation changes because of the ocean and land surfaces have heat capacity (thermal inertial). In other words, insolation is a heating rate which equals to temperature change (tendency) but not the temperature itself. Thus ~~T~~the precipitation change would lag the insolation change by about two months, due to the ocean–atmosphere interaction without other processes. For example, the change of seasonal distribution of NH monsoon precipitation lagged the change of the NH insolation by one month (Yan et al., 2016). Whereas in this study, the Australian monsoon precipitation decreased from March to September and increased from November to February (Fig. 11b), quite different from what it would be (i.e., decrease from September to January and increase from February to August). Meanwhile, the insolation over SH increased during the LGM from April to August, when Australia is in late ~~fall~~ autumn and winter. An increased insolation might make land warmer than ocean thus against the climatology, which may be described by cooler land and warmer ocean in winter. However, the simulated surface temperature reduced more over Australia than the adjacent oceans (Fig. 5a). On the other hand, the synthesis of Wyrwoll et al. (2007) and Liu et al. (2015) indicates the strong convergence rain belt (ITCZ) stays in the north, resulting in more rainfall over Papua New

带格式的: 字体颜色: 自动设置

Guinea and less rainfall over North Australia during those times with low obliquity and high precession. The rain belt stays a little more northerly than that stays in our study, which means the effect of orbital change and thus the insolation change might be suppressed by other factors.

Moreover, the paleoclimate records suggest that it was dry and cool in the Indo-Pacific Warm Pool region during the LGM (Xu et al., 2010). The simulated SST is consistent with the reconstructions. Although in the early austral summer, over the Indian Ocean warm pool, it is cooler over the SH, while over the Pacific warm pool, it is cooler over the NH (Fig. ~~S4~~S7). Such anomalous SST asymmetry may favor the southward shift of the ITCZ over Australia and the southwest Pacific, which might be related to the enhanced austral summer monsoon precipitation. However, the 7MME shows no significant ITCZ shift during the LGM, particularly over the central Australian monsoon region (Fig. ~~S5~~S8). The reconstructions and simulations by McGee et al. (2014) and Mohtadi et al. (2014) also suggested ~~found~~ that there was no significant shift of ITCZ position~~shifted no more than 1° latitude~~ during the LGM.

Therefore, it is the local dynamical processes, instead of the large-scale circulation such as the position of the ITCZ induced by the NH-SH thermal contrast, that might be the key factor influencing the early summer mean precipitation change over the Australian monsoon region during the LGM. To test this synthesis, we conducted two experiments using a newly developed earth system model, the Nanjing University of Information Science and Technology Earth System model version 1 (NESM v1, Cao et al., 2015). The PI control run is designed the same as PMIP3 protocol. The land sea configuration sensitive run (LSM) is the same as the piControl but with the LGM land sea configuration. The two experiments are run 500 years after spin-up, and the last 100 years are used. The changes of the ND mean precipitation and wind field at 1000 hPa between LSM and piControl are similar to the changes derived from the 7MME, i.e. the precipitation is increased and the convergence is strengthened over northern Australia (Fig. 12a). The changes of the 2-m air temperature, SLP and 850 hPa wind field (Fig. 12b, c) are also similar to those results in the 7MME (Fig. 9). It is also cooler over the northwest landmass (western Indonesia–Indochina) and relatively warmer over the southeast landmass (eastern Indonesia–northern Australia) (Fig. 12b). This temperature variation is also accompanied by a northwest–southeast SLP gradient and the strengthened cross equatorial flow converging to north Australia (Fig. 12c). This sensitive simulation confirms that the local dynamical process induced by the land sea configuration to be essential to the Australian monsoonality change.

Although the 7MME simulates strengthened Australian monsoonality, there are uncertainties among individual models. The most notable uncertainty is the increased austral summer (DJF) precipitation. Five out of the 7 models simulate increased DJF mean precipitation over the Australian monsoon region during the LGM (CCSM4, GISS-E2-R, IPSL-CM5A-LR, MIROC-ESM and MRI-CGCM3), while the other two simulate decreased precipitation (CNRM-CM5 and MPI-ESM-P) (Fig. 13), especially over the land area. The wind filed at 850hPa geopotential height shows a cyclonic anomaly pattern over northern Australia in the five models (Fig. 14a), accompanied with a strengthened ascending flow (not shown). While in the other two models, there is no cyclonic wind anomaly over Australia region (Fig. 14b), and the ascending flow is weakened (not shown). The different changes of wind field indicate the different precipitation responses to the LGM boundary conditions in the two model groups.

The austral spring and summer mean 2m-air temperature and SST also change differently in these two model groups. The main differences are located over the tropic Pacific Ocean and the North Atlantic Ocean. It is cooler over high-latitude Northern Atlantic Ocean in the five models, whereas warmer in the two models, mainly in the austral spring (Fig. 15a, 15b). In the austral summer, there is an East-Pacific El Nino like patter in the five models, while there is a Central-Pacific El Nino (CP-El Nino) like pattern in the two models (Fig. 15c, 15d). Studies have shown that the CP-El Nino is related to the Asian-Australian monsoon system (Yu et al. 2009), and would lead to a markedly decreased precipitation in December (Taschetto et al. 2009).

Therefore, the different SST response over Pacific Oceans and North Atlantic Ocean in austral spring and summer in different models might be the key factor that leads to different wind anomalies and thus different Australian monsoon precipitation changes.

带格式的: 缩进: 首行缩进: 3 字符

5 Conclusions

The global mean temperature and water vapor have an overall decrease under the LGM forcings (lower GHG and large ice-sheets). Nevertheless, the simulated Australian monsoon seasonality derived from CMIP5/PMIP3 multi-model ensemble has a distinctive amplification (or the monsoonality is intensified) against the weakened global monsoons elsewhere during the LGM. This study then investigated the possible reasons for this strengthened Australian monsoonality ~~in~~ from both a therm~~al~~o-dynamic~~al~~ and dynamic~~al~~ perspective.

The conclusions are as follows ~~and the relative mechanisms are shown in Fig. 12~~:

1) The Australian monsoon seasonality is strengthened as a result of the enhanced seasonal difference between austral summer and winter, i.e., the increased early summer (ND) mean rainfall and the reduced winter (JJA) mean rainfall. Both the dynamic processes and thermal effects contribute to the precipitation change; however, the dynamic processes have a much stronger contribution than the thermal effects.

2) The Australian winter ~~monsoon~~ (JJA mean) precipitation derived from 7MME decreased ~~by 58 %~~ during the LGM relative to the preindustrial control experiment. The dynamic processes, induced by the enhanced land–ocean thermal contrast, contribute more to ~~a~~ the decreased rainfall ~~of about 48 %~~ through the strengthened divergence over northern Australia (Fig. 16a), whereas the ~~thermal~~ thermodynamic effect (i.e., the reduced atmospheric water vapor due to the lower temperature induced by lower GHGs and present ice-sheets) and evaporation haves ~~a~~ moderate contribution ~~of nearly 20 %~~.

3) For the increased precipitation in early summer (ND) in the 7MME, the local dynamic processes have a positive contribute ~~+29 %~~ion and the therm~~al~~odynamic effect has a negative contributiones ~~−16 %~~. Both the decomposition method and the sensitive simulations show that the dynamic effect plays most important role for the increased rainfall. ~~Correspondingly, the ND precipitation increases by about 13 %.~~ The local dynamic processes are mainly induced by the northwest–southeast thermal contrast between Indochina–western Indonesia and northeastern Australia. The east Indian Ocean–west Pacific Ocean thermal gradient also contributes to these processes (Fig. 16b).

4) The sensitive simulation illustrates that the change in circulation over Australia ~~and South Asia are~~is very likely to be rooted in the enlarged landmasses over the Indochina–western Indonesia and New Guinea, and northern Australia. Another factor contributes to the circulation change might be the asymmetric change between western Pacific Ocean and eastern Indian Ocean. ~~Changes of the land–ocean configuration~~These have ~~has a~~ critical impacts on the thermal gradients that induce changes in the low-level circulation pattern and convergence/divergence.

Note that models have uncertainties, i.e. not all the models simulate an intensified seasonality of Australian monsoon. The different SST responses over Pacific Ocean and Atlantic Ocean in different models to the same external forcings are essential for the model uncertainties. More model-data comparison and inter-model comparison are required to improve model performance.

Our results are based on the equilibrium simulation, representing a ~~synthesized~~ mean state of the Australian monsoon change and its possible mechanisms during the LGM. More simulations with single forcing (such as the SST asymmetry change, the insolation change~~, and the landmass change~~) are required to further understand the effect of each factor and to specifically quantify the contribution of each forcing to the Australian monsoon change.

带格式的: 突出显示

Acknowledgments

We acknowledge Prof. Williams J and the two reviewers for the comments helping to clarify and improve the paper. This research was jointly supported by the National Key Research and Development Program of China (Grant No. 2016YFA0600401), the National Basic Research Program (Grant No. 2015CB953804), the National Natural Science Foundation of China (Grant Nos. 41671197, 41420104002 and 41501210), and the Priority Academic Development Program of Jiangsu Higher Education Institutions (PAPD, Grant No. 164320H116). We acknowledge the World Climate Research Programme's Working Group on Coupled Modeling, which is responsible for the CMIP, and we thank the climate modeling groups for producing and making available their model outputs. For the CMIP, the U.S. Department of Energy's Program for climate model diagnosis and intercomparison provided coordinating support and led the development of software infrastructure in partnership with the Global Organization for Earth System Science Portals. We thank LetPub (www.letpub.com) for its linguistic assistance during the preparation of this manuscript. This is the ESMC publication XXX.

References

Ayliffe, L. K., Gagan, M. K., Zhao, J. X., Drysdale, R. N., Hellstrom, J. C., Hantoro, W. S., Griffiths, M. L., Scott-Gagan, H., St Pierre, E., Cowley, J. A., and Suwargadi, B. W.: Rapid interhemispheric climate links via the Australasian monsoon during the last deglaciation, Nat Commun, 4, 2908, 10.1038/ncomms3908, 2013.

Bayon, G., De Deckker, P., Magee, J. W., Germain, Y., Bermell, S., Tachikawa, K., and Norman, M. D.: Extensive wet episodes in Late Glacial Australia resulting from high-latitude forcings, Scientific Reports, 7, 44054, 10.1038/srep44054, 2017.

~~Bowler, J. M., Gillespie, R., Johnston, H., and Boljkovac, K.: Wind v water: Glacial maximum records from the Willandra Lakes, in: Peopled Landscapes: Archaeological and Biogeographic Approaches to Landscapes, edited by: Haberle, S., and David, B., ANU E Press, Canberra, Australia, 271-296, 2012.~~

Braconnot, P., Otto-Bliesner, B., Harrison, S. P., and al, e.: Results of PMIP2 coupled simulations of the Mid-Holocene and Last Glacial Maximum – Part 2: feedbacks with emphasis on the location of the ITCZ and mid- and high latitudes heat budget, Climate of the Past, 3, 2007.

Braconnot, P., Harrison, S. P., Kageyama, M., Bartlein, P. J., Masson-Delmotte, V., Abe-Ouchi, A., Otto-Bliesner, B., and Zhao, Y.: Evaluation of climate models using palaeoclimatic data, Nature Climate Change, 2, 417-424, 10.1038/nclimate1456, 2012a.

Braconnot, P., Harrison, S. P., Otto-Bliesner, B., Abe-Ouchi, A., Jungclaus, J., and Peterschmitt, J. Y.: The Paleoclimate Modeling Intercomparison Project contribution to CMIP5, CLIVAR Exchanges, 56, 15-19, 2012b.

Broccoli, A. J., Dahl, K. A., and Stouffer, R. J.: Response of the ITCZ to Northern Hemisphere cooling, Geophysical Research Letters, 33(1), L01702, 10.1029/2005gl024546, 2006.

Brown, J. R., Moise, A. F., Colman, R., and Zhang, H.: Will a Warmer World Mean a Wetter or Drier Australian Monsoon? Journal of Climate, 29, 4577-4596, 10.1175/jcli-d-15-0695.1, 2016.

Cao, J., Wang, B., Xiang, B., Li, J., Wu, T., Fu, X., Wu, L., and Min, J.: Major modes of short-term climate variability in the newly developed NUIST Earth System Model (NESM), Advances in Atmospheric Sciences, 32, 585-600, 10.1007/s00376-014-4200-6, 2015.

Chou, C., Neelin, J. D., Chen, C.-A., and Tu, J.-Y.: Evaluating the "Rich-Get-Richer" Mechanism in Tropical Precipitation Change under Global Warming, Journal of Climate, 22, 1982-2005, 10.1175/2008jcli2471.1, 2009.

Cui, X. P.: Quantitative diagnostic analysis of surface rainfall processes by surface rainfall equation. Chinese Journal of Atmospheric Sciences, 33(2), 375–387, 2009.

De Deckker, P., Barrows, T. T., and Rogers, J.: Land–sea correlations in the Australian region: post-glacial onset of the monsoon in northwestern Western Australia, Quaternary Science Reviews, 105, 181-194, 10.1016/j.quascirev.2014.09.030, 2014.

Denniston, R. F., Wyrwoll, K.-H., Asmerom, Y., Polyak, V. J., Humphreys, W. F., Cugley, J., Woods, D., LaPointe, Z., Peota, J., and Greaves, E.: North Atlantic forcing of millennial-scale Indo-Australian monsoon dynamics during the Last Glacial period, Quaternary Science Reviews, 72, 159-168, 10.1016/j.quascirev.2013.04.012, 2013.

Denniston, R. F., Asmerom, Y., Polyak, V. J., Wanamaker, A. D., Ummenhofer, C. C., Humphreys, W. F., Cugley, J., Woods, D., and Lucker, S.: Decoupling of monsoon activity across the northern and southern Indo-Pacific during the Late Glacial, Quaternary Science Reviews, 176, 101-105, 10.1016/j.quascirev.2017.09.014, 2017.

DiNezio, P. N., Timmermann, A., Tierney, J. E., Jin, F.-F., Otto-Bliesner, B., Rosenbloom, N., Mapes, B., Neale, R., Ivanovic, R. F., and Montenegro, A.: The climate response of the Indo-Pacific warm pool to glacial sea level, Paleoceanography, 31, 866-894, 10.1002/2015PA002890, 2016.

DiNezio, P. N., Clement, A., Vecchi, G. A., Soden, B., Broccoli, A. J., Otto-Bliesner, B. L., and Braconnot, P.: The response of the Walker circulation to Last Glacial Maximum forcing: Implications for detection in proxies, Paleoceanography, 26, n/a-n/a, 10.1029/2010pa002083, 2011.

DiNezio, P. N., and Tierney, J. E.: The effect of sea level on glacial Indo-Pacific climate, Nature Geoscience, 6, 485-491, 10.1038/ngeo1823, 2013.

带格式的: Reference, 缩进: 左侧: 0 厘米, 悬挂缩进: 2 字符, 首行缩进: -2 字符, 行距: 1.5 倍行距

Donohoe, A., Marshall, J., Ferreira, D., and McGee, D.: The Relationship between ITCZ Location and Cross-Equatorial Atmospheric Heat Transport: From the Seasonal Cycle to the Last Glacial Maximum, Journal of Climate, 26, 3597-3618, 10.1175/jcli-d-12-00467.1, 2013.

Endo, H., and Kitoh, A.: Thermodynamic and dynamic effects on regional monsoon rainfall changes in a warmer climate, Geophysical Research Letters, 41, 1704-1711, 10.1002/2013gl059158, 2014.

Eroglu, D., McRobie, F. H., Ozken, I., Stemler, T., Wyrwoll, K. H., Breitenbach, S. F., Marwan, N., and Kurths, J.: See-saw relationship of the Holocene East Asian-Australian summer monsoon, Nat Commun, 7, 12929, 10.1038/ncomms12929, 2016.

Hargreaves, J. C., Annan, J. D., Ohgaito, R., Paul, A., and Abe-Ouchi, A.: Skill and reliability of climate model ensembles at the Last Glacial Maximum and mid-Holocene, Climate of the Past, 9, 811-823, 10.5194/cp-9-811-2013, 2013.

Harrison, S. P., Bartlein, P. J., Brewer, S., Prentice, I. C., Boyd, M., Hessler, I., Holmgren, K., Izumi, K., and Willis, K.: Climate model benchmarking with glacial and mid-Holocene climates, Climate Dynamics, 43, 671-688, 10.1007/s00382-013-1922-6, 2014.

Held, I. M., and Soden, B. J.: Robust responses of the hydrological cycle to global warming, Journal of Climate, 19, 5686-5699, 2006.

Hewitt, C., Broccoli, A. J., Mitchell, J. F. B., and Stouffer, R.: A coupled model study of the last glacial maximum: Was part of the North Atlantic relatively warm? Geophys. Res. Lett., 28, 1571-1574, 2001.

Huang, P., Xie, S.-P., Hu, K., Huang, G., and Huang, R.: Patterns of the seasonal response of tropical rainfall to global warming, Nature Geoscience, 6, 357-361, 10.1038/ngeo1792, 2013.

Huffman, G. J., Adler, R. F., Bolvin, D. T., and Gu, G.: Improving the global precipitation record: GPCP Version 2.1, Geophysical Research Letters, 36, 10.1029/2009gl040000, 2009.

Jiang, D., Tian, Z., Lang, X., Kageyama, M., and Ramstein, G.: The concept of global monsoon applied to the last glacial maximum: A multi-model analysis, Quaternary Science Reviews, 126, 126-139, 10.1016/j.quascirev.2015.08.033, 2015.

Jourdain, N. C., Gupta, A. S., Taschetto, A. S., Ummenhofer, C. C., Moise, A. F., and Ashok, K.: The Indo-Australian monsoon and its relationship to ENSO and IOD in reanalysis data and the CMIP3/CMIP5 simulations, Climate Dynamics, 41, 3073-3102, 10.1007/s00382-013-1676-1, 2013.

Kuhnt, W., Holbourn, A., Xu, J., Opdyke, B., De Deckker, P., Rohl, U., and Mudelsee, M.: Southern Hemisphere control on Australian monsoon variability during the late deglaciation and Holocene, Nat Commun, 6, 5916, 10.1038/ncomms6916, 2015.

Li, J., Feng, J., and Li, Y.: A possible cause of decreasing summer rainfall in northeast Australia, International Journal of Climatology, 32, 995-1005, 10.1002/joc.2328, 2012.

Liu, F., Chai, J., Wang, B., Liu, J., Zhang, X., and Wang, Z.: Global monsoon precipitation responses to large volcanic eruptions, Sci Rep, 6, 24331, 10.1038/srep24331, 2016.

Liu, Y., Lo, L., Shi, Z., Wei, K. Y., Chou, C. J., Chen, Y. C., Chuang, C. K., Wu, C. C., Mii, H. S., Peng, Z., Amakawa, H., Burr, G. S., Lee, S. Y., DeLong, K. L., Elderfield, H., and Shen, C. C.: Obliquity pacing of the western Pacific Intertropical Convergence Zone over the past 282,000 years, Nat Commun, 6, 10018, 10.1038/ncomms10018, 2015.

Marshall, A. G., and Lynch, A. H.: Time-slice analysis of the Australian summer monsoon during the late Quaternary using the Fast Ocean Atmosphere Model, Journal of Quaternary Science, 21, 789-801, 10.1002/jqs.1063, 2006.

Marshall, A. G., and Lynch, A. H.: The sensitivity of the Australian summer monsoon to climate forcing during the late Quaternary, Journal of Geophysical Research, 113, 10.1029/2007jd008981, 2008.

McGee, D., Donohoe, A., Marshall, J., and Ferreira, D.: Changes in ITCZ location and cross-equatorial heat transport at the Last Glacial Maximum, Heinrich Stadial 1, and the mid-Holocene, Earth and Planetary Science Letters, 390, 69-79, 10.1016/j.epsl.2013.12.043, 2014.

Miller, G. H., Fogel, M. L., Magee, J. W., and Gagan, M. K.: Disentangling the impacts of climate and human colonization on the flora and fauna of the Australian arid zone over the past 100 ka using stable isotopes in avian eggshell, Quaternary Science Reviews, 151, 27-57, 10.1016/j.quascirev.2016.08.009, 2016.

Mohtadi, M., Prange, M., Oppo, D. W., De Pol-Holz, R., Merkel, U., Zhang, X., Steinke, S., and Lückge, A.: North Atlantic forcing of tropical Indian Ocean climate, Nature, 509, 76, 10.1038/nature13196, 2014.

Petherick, L., Bostock, H., Cohen, T. J., Fitzsimmons, K., Tibby, J., Fletcher, M. S., Moss, P., Reeves, J., Mooney, S., Barrows, T., Kemp, J., Jansen, J., Nanson, G., and Dosseto, A.: Climatic records over the past 30 ka from temperate Australia – a synthesis from the Oz-INTIMATE workgroup, Quaternary Science Reviews, 74, 58-77, 10.1016/j.quascirev.2012.12.012, 2013.

Reeves, J. M., Barrows, T. T., Cohen, T. J., Kiem, A. S., Bostock, H. C., Fitzsimmons, K. E., Jansen, J. D., Kemp, J., Krause, C., Petherick, L., and Phipps, S. J.: Climate variability over the last 35,000 years recorded in marine and terrestrial archives in the Australian region: an OZ-INTIMATE compilation, Quaternary Science Reviews, 74, 21-34, 10.1016/j.quascirev.2013.01.001, 2013a.

Reeves, J. M., Bostock, H. C., Ayliffe, L. K., Barrows, T. T., De Deckker, P., Devriendt, L. S., Dunbar, G. B., Drysdale, R. N., Fitzsimmons, K. E., Gagan, M. K., Griffiths, M. L., Haberle, S. G., Jansen, J. D., Krause, C., Lewis, S., McGregor, H. V., Mooney, S. D., Moss, P., Nanson, G. C., Purcell, A., and van der Kaars, S.: Palaeoenvironmental change in tropical Australasia over the last 30,000 years – a synthesis by the OZ-INTIMATE group, Quaternary Science Reviews, 74, 97-114, 10.1016/j.quascirev.2012.11.027, 2013b.

Rojas, M.: Sensitivity of Southern Hemisphere circulation to LGM and 4 × CO2 climates, Geophysical Research Letters, 40, 965-970, 10.1002/grl.50195, 2013.

Seager, R., Naik, N., and Vecchi, G. A.: Thermodynamic and Dynamic Mechanisms for Large-Scale Changes in the Hydrological Cycle in Response to Global Warming*, Journal of Climate, 23, 4651-4668, 10.1175/2010jcli3655.1, 2010.

Taylor, K. E., Stouffer, R. J., and Meehl, G. A.: An Overview of CMIP5 and the Experiment Design, Bulletin of the American Meteorological Society, 93, 485-498, 10.1175/bams-d-11-00094.1, 2012.

Tharammal, T., Paul, A., Merkel, U., and Noone, D.: Influence of Last Glacial Maximum boundary conditions on the global water isotope distribution in an atmospheric general

circulation model, Climate of the Past, 9, 789-809, 10.5194/cp-9-789-2013, 2013.~~Treble, P. C., Baker, A., Ayliffe, L. K., Cohen, T. J., Hellstrom, J. C., Gagan, M. K., Frisia, S., Drysdale, R. N., and Griffiths, A. D.: Hydroclimate of the Last Glacial Maximum and deglaciation in southern Australia's arid margin interpreted from speleothem records (23–15 ka), Climate of the Past, 13, 667-687, 2017.~~

~~Treble, P. C., Baker, A., Ayliffe, L. K., Cohen, T. J., Hellstrom, J. C., Gagan, M. K., Frisia, S., Drysdale, R. N., and Griffiths, A. D.: Hydroclimate of the Last Glacial Maximum and deglaciation in southern Australia's arid margin interpreted from speleothem records (23–15 ka), Climate of the Past, 13, 667-687, 2017.~~

Turney, C. S. M., Haberle, S., Fink, D., Kershaw, A. P., Barbetti, M., Barrows, T. T., Black, M., Cohen, T. J., Corrège, T., Hesse, P. P., Hua, Q., Johnston, R., Morgan, V., Moss, P., Nanson, G., van Ommen, T., Rule, S., Williams, N. J., Zhao, J. X., D'Costa, D., Feng, Y. X., Gagan, M., Mooney, S., and Xia, Q.: Integration of ice-core, marine and terrestrial records for the Australian Last Glacial Maximum and Termination: a contribution from the OZ INTIMATE group, Journal of Quaternary Science, 21, 751-761, 10.1002/jqs.1073, 2006.

Wang, B., and Ding, Q.: Global monsoon: Dominant mode of annual variation in the tropics, Dynamics of Atmospheres and Oceans, 44, 165-183, 10.1016/j.dynatmoce.2007.05.002, 2008.

Wang, P. X., Wang, B., Cheng, H., Fasullo, J., Guo, Z., Kiefer, T., and Liu, Z.: The global monsoon across time scales: Mechanisms and outstanding issues, Earth-Science Reviews, 10.1016/j.earscirev.2017.07.006, 2017.

Williams, A. N., Ulm, S., Cook, A. R., Langley, M. C., and Collard, M.: Human refugia in Australia during the Last Glacial Maximum and Terminal Pleistocene: a geospatial analysis of the 25–12 ka Australian archaeological record, Journal of Archaeological Science, 40, 4612-4625, 10.1016/j.jas.2013.06.015, 2013.

Wyrwoll, K.-H., Liu, Z., Chen, G., Kutzbach, J. E., and Liu, X.: Sensitivity of the Australian summer monsoon to tilt and precession forcing, Quaternary Science Reviews, 26, 3043-3057, 10.1016/j.quascirev.2007.06.026, 2007.

Wyrwoll, K.-H., Hopwood, J. M., and Chen, G.: Orbital time-scale circulation controls of the Australian summer monsoon: a possible role for mid-latitude Southern Hemisphere forcing? Quaternary Science Reviews, 35, 23-28, 10.1016/j.quascirev.2012.01.003, 2012.

Xie, P., and Arkin, P.: Global precipitation: a 17-year monthly analysis based on Gauge Obseravations, satellite estimates, and numerical model outputs, Bulletin of the American Meteorological Society, 78, 2539-2558, 1997.

Xu, J., Kuhnt, W., Holbourn, A., Regenberg, M., and Andersen, N.: Indo-Pacific Warm Pool variability during the Holocene and Last Glacial Maximum, Paleoceanography, 25, 10.1029/2010pa001934, 2010.

Yan, M., Wang, B., and Liu, J.: Global monsoon change during the Last Glacial Maximum: a multi-model study, Climate Dynamics, 47, 359-374, 10.1007/s00382-015-2841-5, 2016.

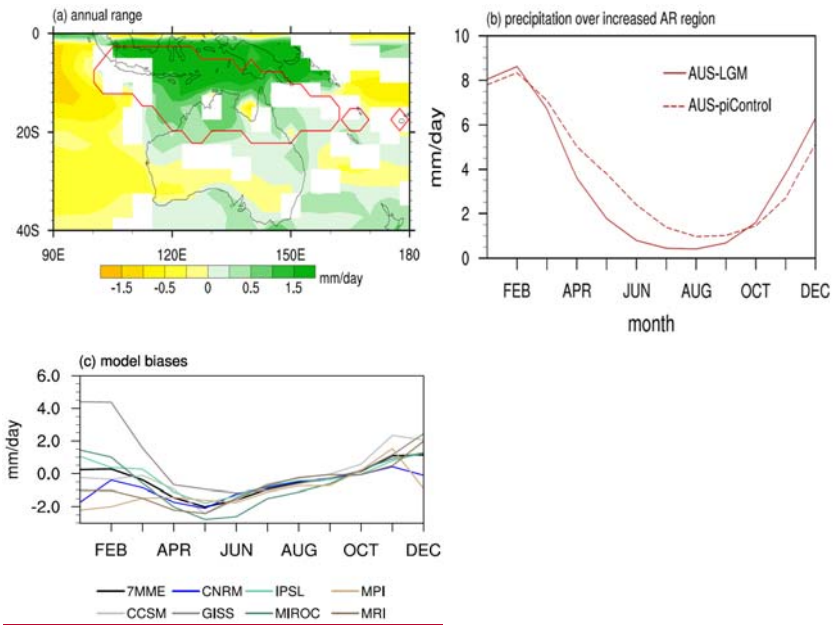

Figure 1 (**a**) Spatial distribution of changes in the annual range (AR) of precipitation measured by the difference between LGME and piControl, ~~and~~ (**b**) ~~annual cycle~~seasonal distribution of the precipitation in the increased AR area (20°S-5°S, 120°E-145°E)~~annual range region over the Australian monsoon~~, and (c) seasonal distribution of the precipitation differences in the increased AR area derived from 7 MME (black line) and each model (colored lines). The red solid line in (**a**) encloses the Australian monsoon rainfall domain. The dashed (solid) line in (**b**) denotes the seasonal distribution of precipitation derived from the piControl (LGME) run. Only those areas where signal-to-noise ratio exceeds one are plotted in (**a**).

带格式的: 字体: 小四

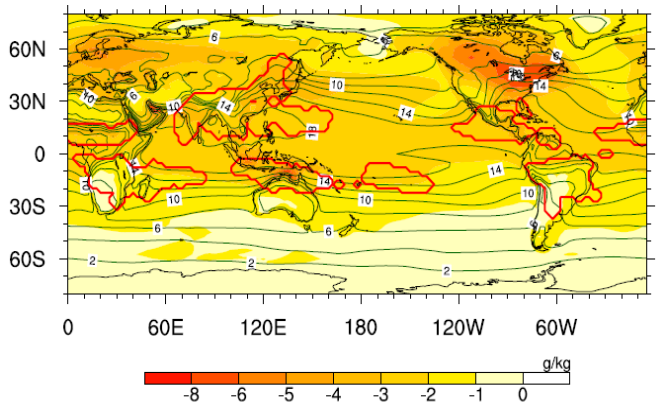

Figure 2 Difference of JJA mean surface specific humidity between LGME and piControl (shaded). The green contours denote the climatology derived from piControl. The red lines enclose the monsoon domains. Only those areas where signal-to-noise ratio exceeds one are plotted.

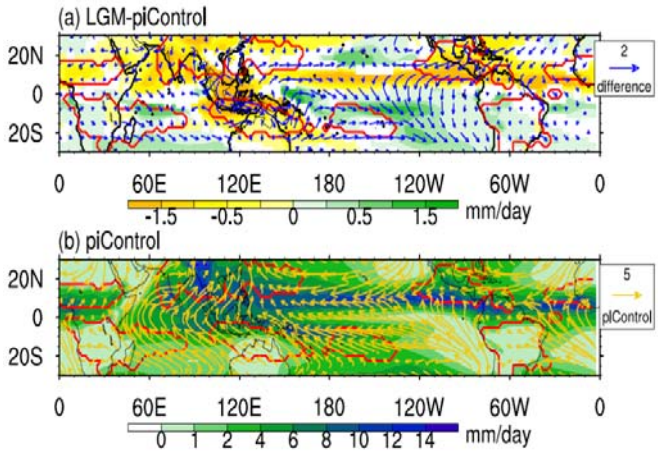

Figure 3 (**a**) JJA mean precipitation (shading) difference and surface wind (vectors) difference between LGME and piControl, and (**b**) the climatology of JJA mean precipitation (shading) and surface wind (vectors) derived from piControl. The red lines enclose the monsoon domains. The thick black lines in (**a**) denote the coastal lines in LGME, and the thin black lines denote the

coastal lines in piControl. Only those areas where signal-to-noise ratio exceeds one are plotted in (**a**).

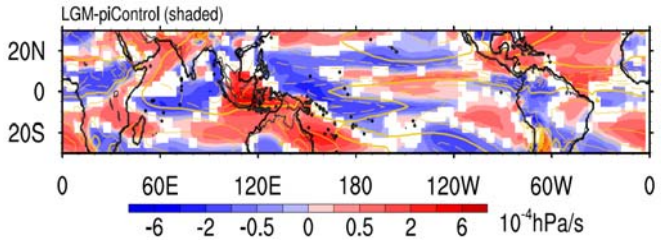

Figure 4 The difference of JJA mean vertical velocity at 500 hPa between LGME and piControl (in shading) and the corresponding climatology derived from piControl (yellow contours). The thick black lines denote the coastal lines in LGME, and the thin black lines denote the coastal lines in piControl. Only those areas where signal-to-noise ratio exceeds one are plotted in the difference pattern.

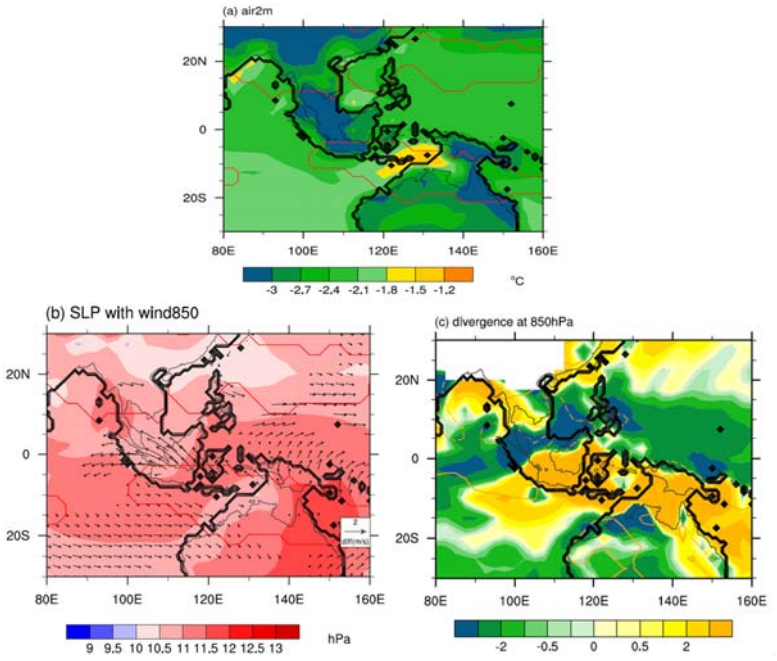
(a) air2m
20N
0
20S
80E
100E
120E
140E
160E
-3 -2.7 -2.4 -2.1 -1.8 -1.5 -1.2
°C
(b) SLP with wind850
9 9.5 10 10.5 11 11.5 12 12.5 13
hPa
(c) divergence at 850hPa
-2 -0.5 0 0.5 2

711

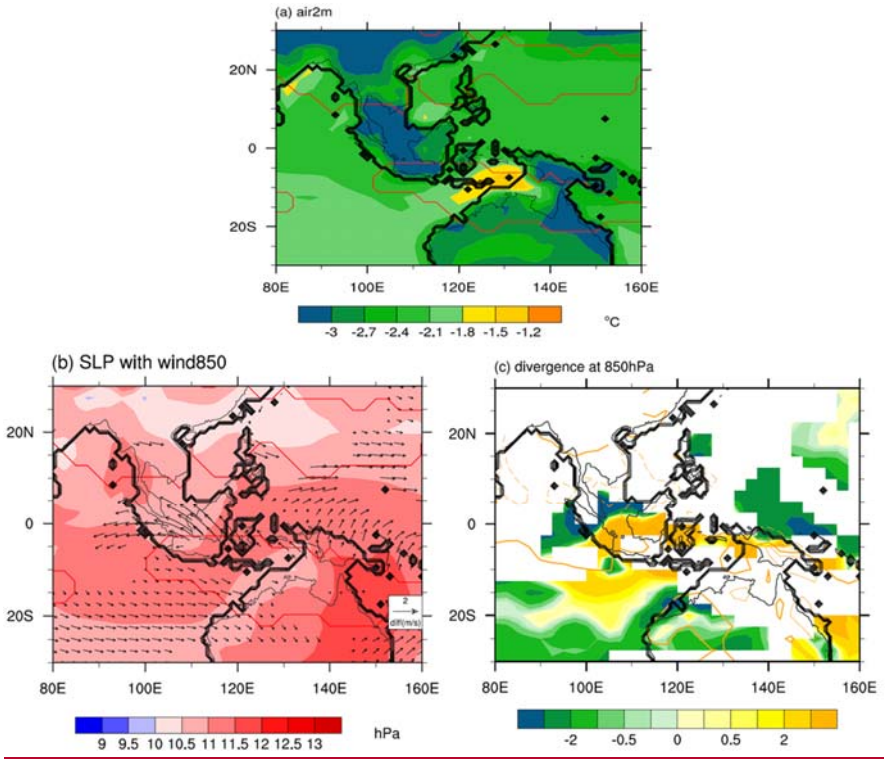

Figure 5 JJA mean (**a**) surface air temperature, (**b**) sea level pressure (shading) with 850 hPa wind (vector), and (**c**) 850 hPa divergence differences between LGME and piControl. The red lines in (**a**) and (**b**) enclose the monsoon domains. The orange lines in (**c**) represent the climatology derived from piControl. The thick black lines denote the coastal lines in LGME, and the thin black lines denote the coastal lines in piControl. Only those areas where signal-to-noise ratio exceeds one are plotted.

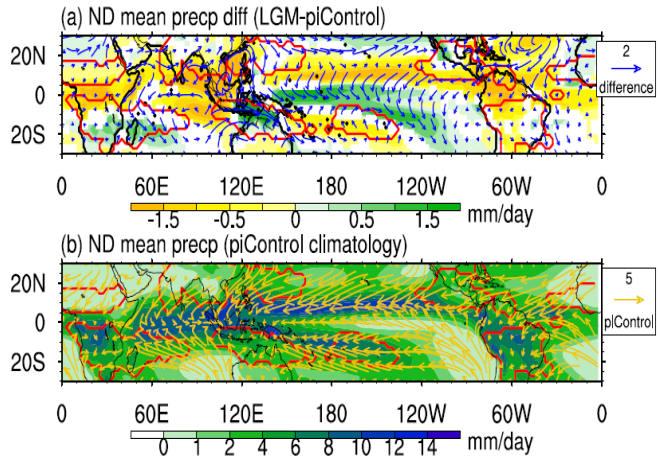

Figure 6 (**a**) ND mean precipitation (shading) difference and surface wind (vectors) difference between LGME and piControl, and (**b**) the climatology of ND mean precipitation (shading) and surface wind (vectors) derived from piControl. The red lines enclose the monsoon domains. The thick black lines in (**a**) denote the coastal lines in LGME, and the thin black lines denote the coastal lines in piControl. Only those areas where signal-to-noise ratio exceeds one are plotted in (**a**).

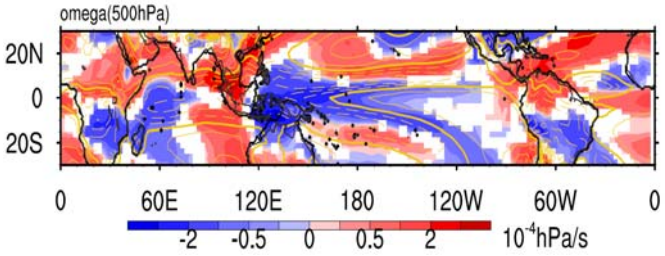

Figure 7 The difference of the ND mean vertical velocity at 500 hPa between LGME and piControl (in shading) and the corresponding climatology derived from piControl (yellow contours). The thick black lines denote the coastal lines in LGME, and the thin black lines denote the coastal lines in piControl. Only those areas where signal-to-noise ratio exceeds one are plotted in the difference pattern.

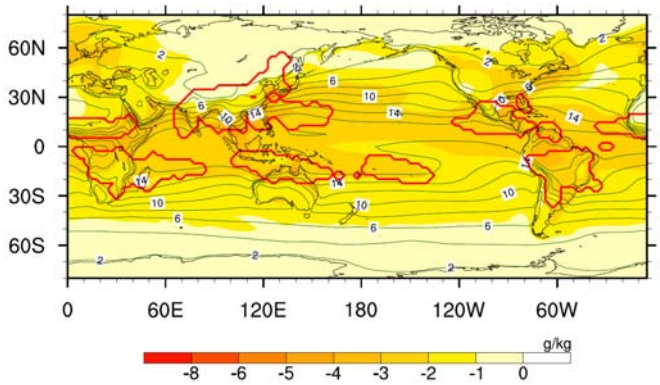

Figure 8 Difference of ND mean surface specific humidity between LGME and piControl (shaded). The green contours denote the climatology derived from piControl. The red lines enclose the monsoon domains. Only those areas where signal-to-noise ratio exceeds one are plotted.

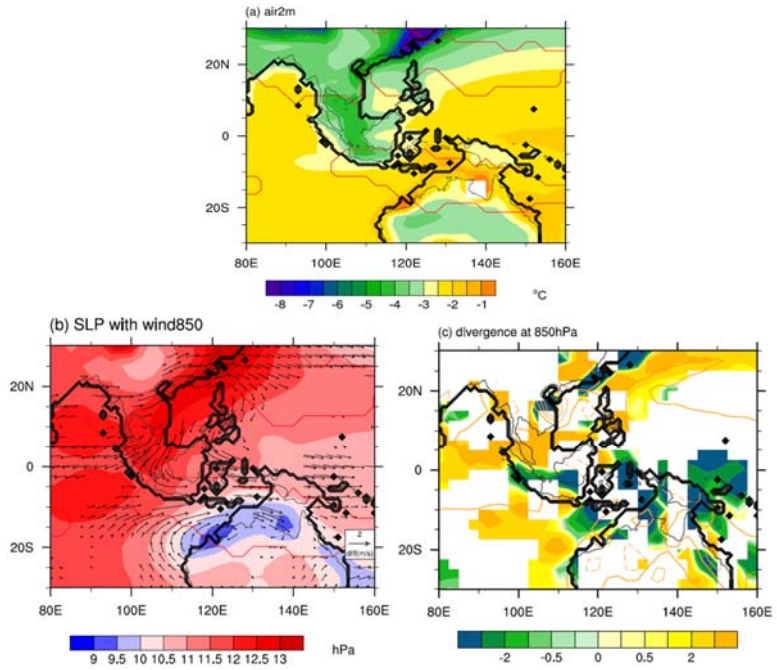

741

742 **Figure 9** ND mean (**a**) surface air temperature, (**b**) sea level pressure (shading) with 850 hPa
743 wind (vector), and (**c**) 850 hPa divergence difference between LGME and piControl (shading).
744 The red lines in (**a**) and (**b**) enclose the monsoon domains. The orange lines in (**c**) represents the
745 climatology derived from piControl. The thick black lines denote the coastal lines in LGME, and
746 the thin black lines denote the coastal lines in piControl. Only those areas where signal-to-noise
747 ratio exceeds one are plotted.

748

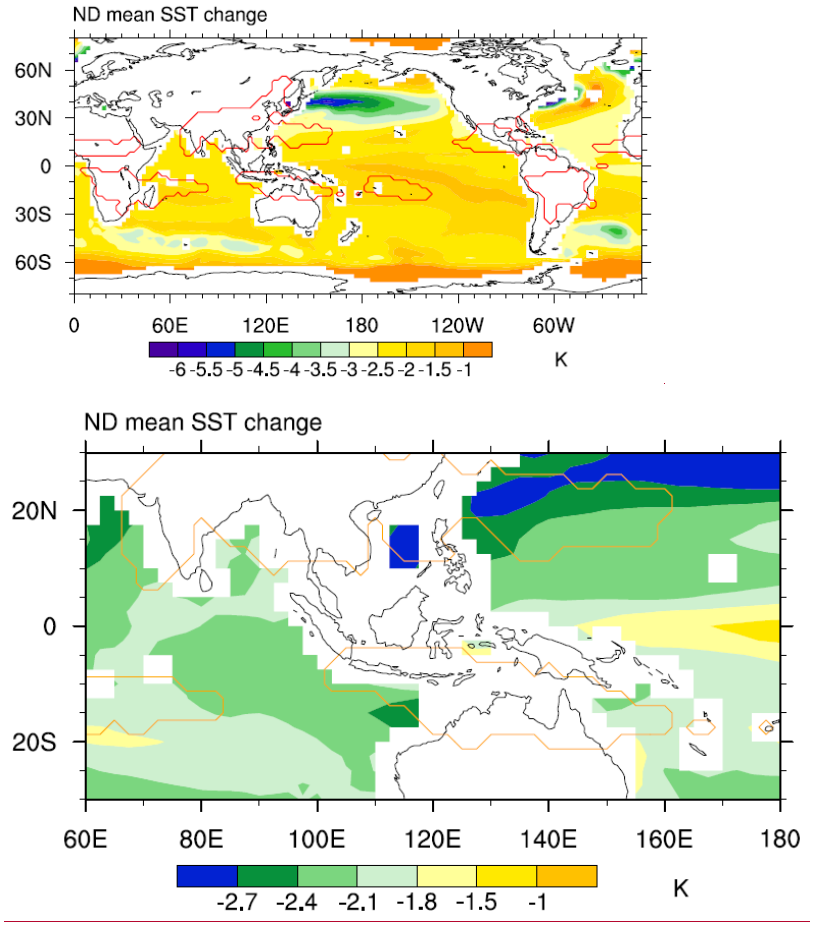

Figure 10 ND mean SST difference between LGME and piControl. The red lines enclose the monsoon domains. Only those areas where signal-to-noise ratio exceeds one are plotted.

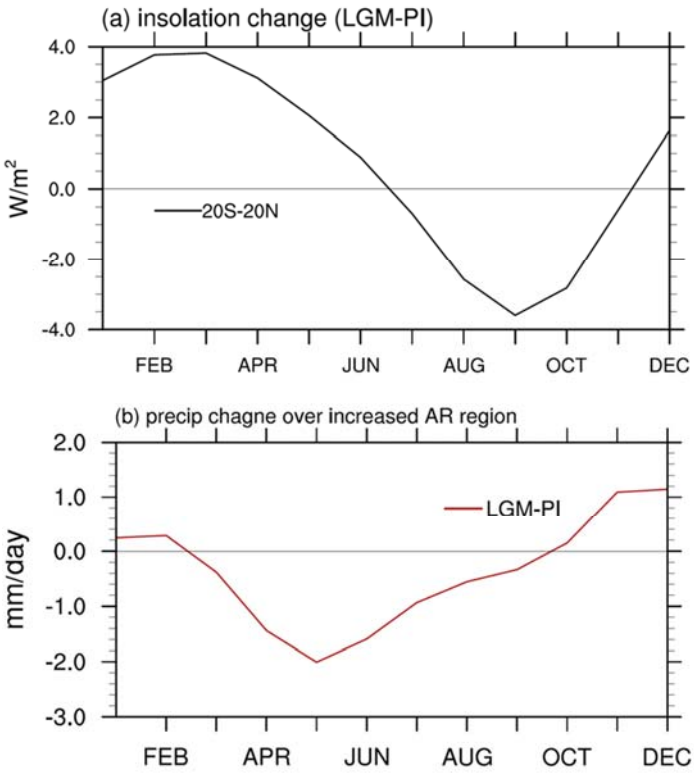

Figure 11 Seasonal distribution of (**a**) insolation change between 20°S and 20°N, and (**b**) precipitation change over the increased AR region as indicated in Fig. 1b (20°S-5°S, 120°E-145°E)~~central Australian monsoon region~~. The changes are calculated by the LGM value minus the PI value.

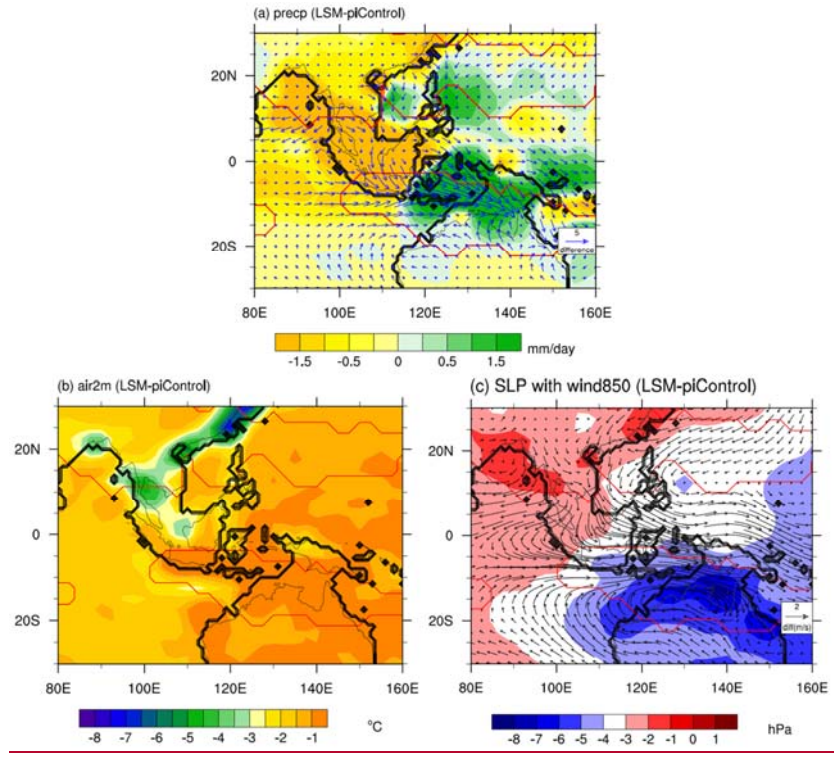

Figure 12 ND mean (a) precipitation (shading) with 1000 hPa wind (vector), (b) surface air temperature, and (c) sea level pressure (shading) with 850 hPa wind (vector) difference between land sea configuration experiment (LSM) and piControl. The red lines enclose the monsoon domains. The thick black lines denote the coastal lines in LSM, and the thin black lines denote the coastal lines in piControl.

带格式的: 字体: 加粗

带格式的: 缩进: 首行缩进: 0 厘米

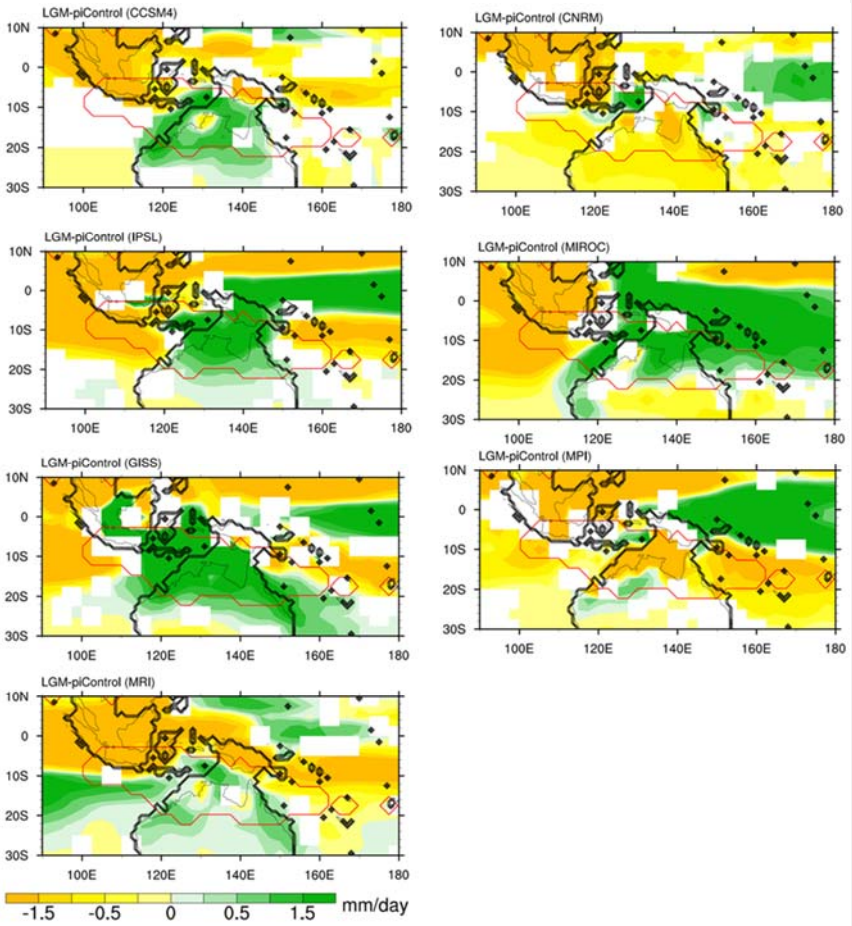

Figure 13 DJF mean precipitation difference between LGME and piControl derived from each model. The red lines enclose the monsoon domains. Only those areas where signal-to-noise ratio exceeds one are plotted.

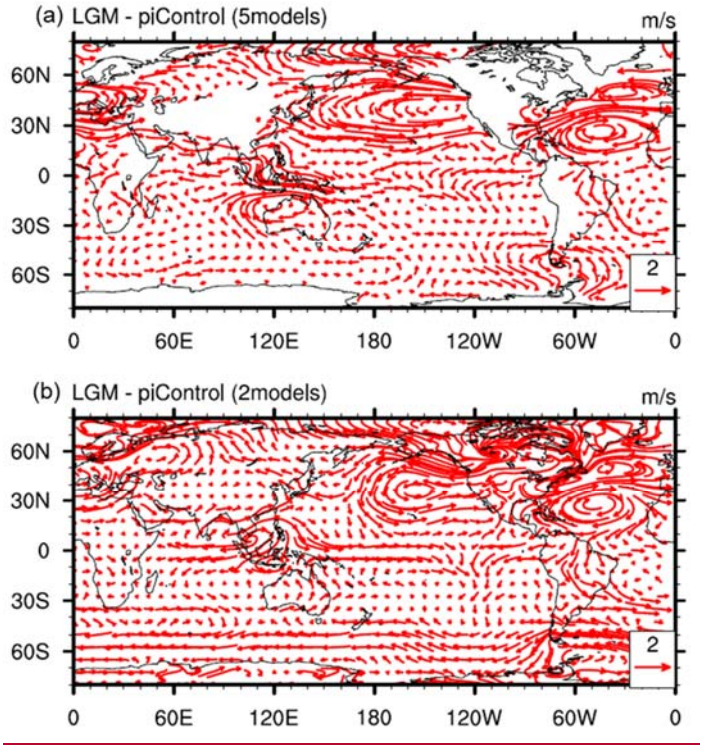

780

781 **Figure 14** DJF mean 850hPa wind differences between LGME and piControl derived from (a)
782 the five models and (b) the two models. Only those areas where signal-to-noise ratio exceeds one
783 are plotted.

784

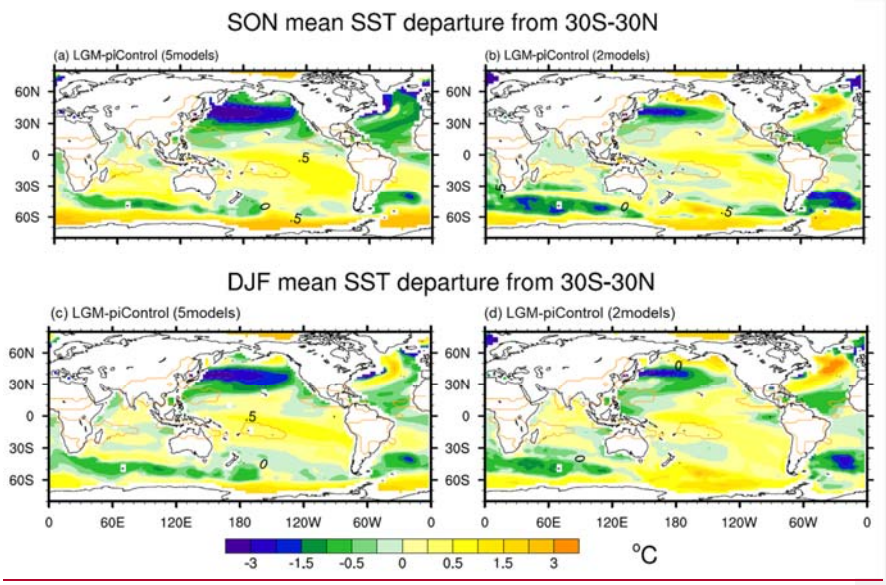

Figure 15 SON mean (a)-(b) and DJF mean (c)-(d) SST differences between LGME and piControl derived from (a), (c) the five models and (b), (d) the two models. Only those areas where signal-to-noise ratio exceeds one are plotted. The area average of tropical (30°S-30°N) SST change is distracted to make it clearer to illustrate the regional differences.

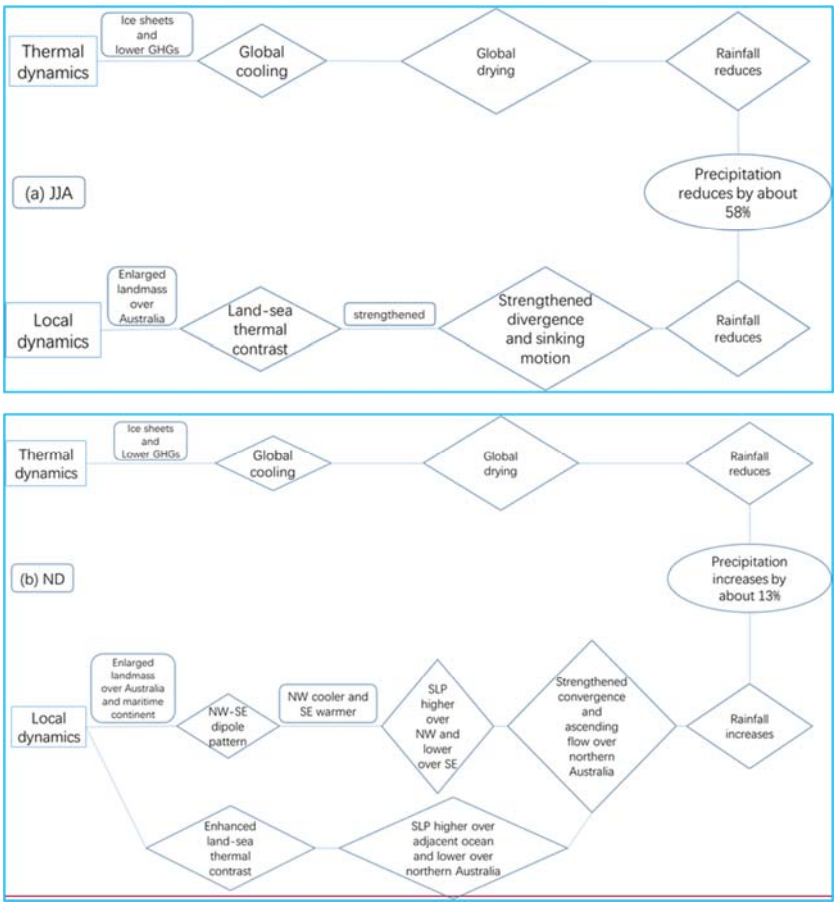
Thermal dynamics
Ice sheets and lower GHGs
Global cooling
Global drying
Rainfall reduces
(a) JJA
Precipitation reduces by about 58%
Local dynamics
Enlarged landmass over Australia
Land-sea thermal contrast
strengthened
Strengthened divergence and sinking motion
Rainfall reduces
Thermal dynamics
Ice sheets and Lower GHGs
Global cooling
Global drying
Rainfall reduces
(b) ND
Precipitation increases by about 13%
Local dynamics
Enlarged landmass over Australia and maritime continent
NW-SE dipole pattern
NW cooler and SE warmer
SLP higher over NW and lower over SE
Strengthened convergence and ascending flow over northern Australia
Rainfall increases
Enhanced land-sea thermal contrast
SLP higher over adjacent ocean and lower over northern Australia

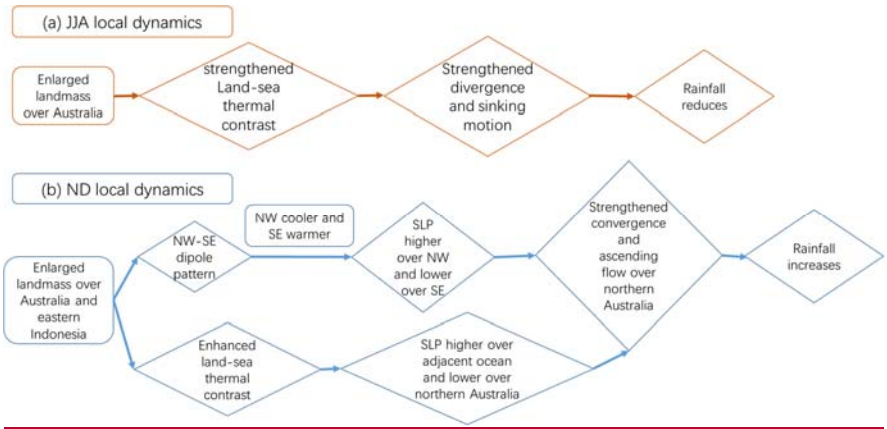

Figure ~~12~~ 16 Mechanisms of Australian monsoon precipitation change (**a**) in JJA, and (**b**) in ND during the LGM, in ~~thermal dynamics and~~ the local dynamics perspective~~s~~.

Table 1 CMIP5/PMIP3 models and experiments used in this study.

Model	Institution	piControl Time span (years)	LGME Time span (years)	Spatial resolution for atmospheric module ~~Lat~~ Lon × ~~Lon~~ Lat Grids	Spatial resolution for oceanic module Lon × Lat Grids
CCSM4	National Centre for Atmospheric Research (NCAR)	501	101	288 × 192	320×384
CNRM-CM5	Centre National de Recherches Meteorologiques/Centre Europeen de Recherche et Formation Avancees en Calcul Scientifique (CNRM-CERFACS)	850	200	256 × 128	362×292
GISS-E2-R	NASA Goddard Institute for Space Studies (NASA GISS)	1200	100	144 × 90	288×180
IPSL-CM5A-LR	Institute Pierre-Simon Laplace (IPSL)	1000	200	96 × 95	182×149
MIROC-ESM	Atmosphere and Ocean Research Institute, University of Tokyo, National Institute for Environmental studies, and Japan Agency for Marine-Earth Science and Technology	531	100	128 × 64	256×192
MPI-ESM-P	Max Planck Institute for Meteorology	1156	100	196 × 98	256×220
MRI-CGCM3	Meteorological Research Institute (MRI)	500	100	320 × 160	364×368

Table 2 Main changed boundary conditions used for the piControl and LGME experiments.

	piControl	**LGME**
Orbital parameters	Eccentricity = 0.016724	Eccentricity = 0.018994
	Obliquity = 23.446°	Obliquity = 22.949°
	Angular precession = 102.04°	Angular precession = 114.42°
Trace gases	CO_2 = 280 ppm	CO_2 = 185 ppm
	CH_4 = 650 ppb	CH_4 = 350 ppb
	N_2O = 270 ppb	N_2O = 200 ppb
Ice sheets	Modern	Provided by ICE-6G v2 (Peltier, 2009)

Land surface elevation and coastlines	Modern	Provided by PMIP3

Table 3 Annual mean, austral summer (DJF) mean and annual range of precipitation change over the region of (20°S-~~EQ~~5°S, ~~115~~120°E-145°E). The area averaged value is calculated based on the areas where S2N ratio exceed one.

Model	**Annual mean (mm/day)**	**Summer mean (mm/day)**	**Annual range (mm/day)**
CCSM4	-0.14	0.49	1.36
CNRM-CM5	-0.78	-0.74	0.12
GISS-E2-R	0.79	3.74	4.66
IPSL-CM5A-LR	-0.17	0.90	1.82
MIROC-ESM	-0.53	1.25	3.17
MPI-ESM-P	-1.02	-1.71	-0.52
MRI-CGCM3	-0.68	-0.01	0.85
7MME	-0.36	0.56	1.61

带格式表格

带格式的: 字体: (中文) +中文正文 (宋体)

第 7 页: [1] 带格式的 **myan** **2018/8/5 17:14:00**

字体: (中文) 宋体, 字体颜色: 自动设置, (中文) 中文(中国)

第 7 页: [1] 带格式的 **myan** **2018/8/5 17:14:00**

字体: (中文) 宋体, 字体颜色: 自动设置, (中文) 中文(中国)

第 7 页: [2] 带格式的 **myan** **2018/8/5 17:14:00**

字体颜色: 自动设置

第 7 页: [2] 带格式的 **myan** **2018/8/5 17:14:00**

字体颜色: 自动设置

第 7 页: [2] 带格式的 **myan** **2018/8/5 17:14:00**

字体颜色: 自动设置

第 7 页: [2] 带格式的 **myan** **2018/8/5 17:14:00**

字体颜色: 自动设置

第 7 页: [2] 带格式的 **myan** **2018/8/5 17:14:00**

字体颜色: 自动设置

第 7 页: [2] 带格式的 **myan** **2018/8/5 17:14:00**

字体颜色: 自动设置

第 7 页: [3] 带格式的 **myan** **2018/8/5 17:14:00**

字体颜色: 自动设置

第 7 页: [3] 带格式的 **myan** **2018/8/5 17:14:00**

字体颜色: 自动设置

第 7 页: [3] 带格式的 **myan** **2018/8/5 17:14:00**

字体颜色: 自动设置

第 7 页: [3] 带格式的 **myan** **2018/8/5 17:14:00**

字体颜色: 自动设置

第 7 页: [3] 带格式的 **myan** **2018/8/5 17:14:00**

字体颜色: 自动设置

第 7 页: [3] 带格式的 **myan** **2018/8/5 17:14:00**

字体颜色: 自动设置

第 7 页: [3] 带格式的 myan 2018/8/5 17:14:00

字体颜色: 自动设置

第 7 页: [3] 带格式的 myan 2018/8/5 17:14:00

字体颜色: 自动设置

第 7 页: [3] 带格式的 myan 2018/8/5 17:14:00

字体颜色: 自动设置

第 7 页: [3] 带格式的 myan 2018/8/5 17:14:00

字体颜色: 自动设置

第 7 页: [3] 带格式的 myan 2018/8/5 17:14:00

字体颜色: 自动设置

第 7 页: [3] 带格式的 myan 2018/8/5 17:14:00

字体颜色: 自动设置

第 7 页: [3] 带格式的 myan 2018/8/5 17:14:00

字体颜色: 自动设置

第 7 页: [4] 带格式的 myan 2018/8/5 17:15:00

字体: (中文) 宋体, 字体颜色: 自动设置, (中文) 中文(中国)

第 7 页: [4] 带格式的 myan 2018/8/5 17:15:00

字体: (中文) 宋体, 字体颜色: 自动设置, (中文) 中文(中国)

第 7 页: [4] 带格式的 myan 2018/8/5 17:15:00

字体: (中文) 宋体, 字体颜色: 自动设置, (中文) 中文(中国)

第 7 页: [5] 带格式的 myan 2018/8/5 17:15:00

字体: (中文) 宋体, 字体颜色: 自动设置, (中文) 中文(中国)

第 7 页: [5] 带格式的 myan 2018/8/5 17:15:00

字体: (中文) 宋体, 字体颜色: 自动设置, (中文) 中文(中国)

第 7 页: [5] 带格式的 myan 2018/8/5 17:15:00

字体: (中文) 宋体, 字体颜色: 自动设置, (中文) 中文(中国)

第 7 页: [5] 带格式的	myan	2018/8/5 17:15:00

字体: (中文) 宋体, 字体颜色: 自动设置, (中文) 中文(中国)

第 7 页: [6] 带格式的	myan	2018/8/5 17:14:00

字体颜色: 自动设置

第 7 页: [6] 带格式的	myan	2018/8/5 17:14:00

字体颜色: 自动设置

第 7 页: [6] 带格式的	myan	2018/8/5 17:14:00

字体颜色: 自动设置

第 7 页: [6] 带格式的	myan	2018/8/5 17:14:00

字体颜色: 自动设置

第 7 页: [6] 带格式的	myan	2018/8/5 17:14:00

字体颜色: 自动设置

第 7 页: [6] 带格式的	myan	2018/8/5 17:14:00

字体颜色: 自动设置

第 7 页: [6] 带格式的	myan	2018/8/5 17:14:00

字体颜色: 自动设置

第 7 页: [6] 带格式的	myan	2018/8/5 17:14:00

字体颜色: 自动设置

第 7 页: [6] 带格式的	myan	2018/8/5 17:14:00

字体颜色: 自动设置

第 7 页: [6] 带格式的	myan	2018/8/5 17:14:00

字体颜色: 自动设置

第 7 页: [6] 带格式的	myan	2018/8/5 17:14:00

字体颜色: 自动设置

第 7 页: [6] 带格式的	myan	2018/8/5 17:14:00

字体颜色: 自动设置

第 7 页: [7] 带格式的	myan	2018/8/5 17:15:00

字体: (中文) 宋体, 字体颜色: 自动设置, (中文) 中文(中国)

第 7 页: [7] 带格式的	myan	2018/8/5 17:15:00

字体: (中文) 宋体, 字体颜色: 自动设置, (中文) 中文(中国)

第 7 页: [7] 带格式的	myan	2018/8/5 17:15:00

字体: (中文) 宋体, 字体颜色: 自动设置, (中文) 中文(中国)

第 7 页: [8] 带格式的	myan	2018/8/5 17:15:00

字体: (中文) 宋体, 字体颜色: 自动设置, (中文) 中文(中国)

第 7 页: [8] 带格式的	myan	2018/8/5 17:15:00

字体: (中文) 宋体, 字体颜色: 自动设置, (中文) 中文(中国)

第 7 页: [9] 带格式的	myan	2018/8/5 17:15:00

字体: (中文) 宋体, 字体颜色: 自动设置, (中文) 中文(中国)

第 7 页: [9] 带格式的	myan	2018/8/5 17:15:00

字体: (中文) 宋体, 字体颜色: 自动设置, (中文) 中文(中国)

第 7 页: [9] 带格式的	myan	2018/8/5 17:15:00

字体: (中文) 宋体, 字体颜色: 自动设置, (中文) 中文(中国)

第 7 页: [10] 带格式的	myan	2018/8/5 17:15:00

字体: (中文) 宋体, 字体颜色: 自动设置, (中文) 中文(中国)

第 7 页: [10] 带格式的	myan	2018/8/5 17:15:00

字体: (中文) 宋体, 字体颜色: 自动设置, (中文) 中文(中国)

第 7 页: [10] 带格式的	myan	2018/8/5 17:15:00

字体: (中文) 宋体, 字体颜色: 自动设置, (中文) 中文(中国)

第 7 页: [10] 带格式的	myan	2018/8/5 17:15:00

字体: (中文) 宋体, 字体颜色: 自动设置, (中文) 中文(中国)

第 7 页: [10] 带格式的	myan	2018/8/5 17:15:00

字体: (中文) 宋体, 字体颜色: 自动设置, (中文) 中文(中国)

第 7 页: [10] 带格式的	myan	2018/8/5 17:15:00

字体: (中文) 宋体, 字体颜色: 自动设置, (中文) 中文(中国)

第 7 页: [11] 带格式的 **myan** **2018/8/5 17:19:00**

字体: Times New Roman

第 7 页: [11] 带格式的 **myan** **2018/8/5 17:19:00**

字体: Times New Roman

第 7 页: [12] 带格式的 **myan** **2018/8/5 17:14:00**

字体颜色: 自动设置

第 7 页: [12] 带格式的 **myan** **2018/8/5 17:14:00**

字体颜色: 自动设置

第 7 页: [12] 带格式的 **myan** **2018/8/5 17:14:00**

字体颜色: 自动设置

第 7 页: [13] 带格式的 **myan** **2018/8/5 17:14:00**

字体颜色: 自动设置

第 7 页: [13] 带格式的 **myan** **2018/8/5 17:14:00**

字体颜色: 自动设置

第 7 页: [13] 带格式的 **myan** **2018/8/5 17:14:00**

字体颜色: 自动设置

第 7 页: [13] 带格式的 **myan** **2018/8/5 17:14:00**

字体颜色: 自动设置

第 7 页: [13] 带格式的 **myan** **2018/8/5 17:14:00**

字体颜色: 自动设置